Echelles: scalar, electromagnetic, and real-groove properties

E. Loewen, D. Maystre, E. Popov, and L. Tsonev

For lack of alternatives, echelle-grating diffraction behavior has in the past been modeled on scalar theory, despite observations that indicate significant deviations. To resolve this difficulty a detailed experimental, theoretical, and numerical study is performed for several echelles that work at low (8–13), medium (35–55), high (84–140), and very-high (to 660) diffraction orders. Noticeable deviations from the scalar model were detected both experimentally and numerically, on the basis of electromagnetic theory: (1) the shift of the observed blaze position was shown to decrease with the wavelength-to-period ratio, and it tends to zero more rapidly than the decrease of the maximum width, so that the TE- and TM-plane responses tend to merge into each other; (2) cut-off effects (Rayleigh anomalies) were found to play a significant role for high groove angles, where passing-off orders are close to the blaze order. A possibility for evaluation of the blaze angle from angular, rather than from spectral, measurements is discussed.Several reasons for the differences between real and ideal echelles (material-index deviations, profile deformations, and groove-angle errors) are analyzed, and their effects on the performance of echelles is studied.

1. Introduction

The concept of echelles is due mainly to Harrison,[1] who conceived of them as highly useful devices intermediate between a Michelson echelon and an ordinary grating, often termed an echelette. Echelons have virtually disappeared, because they are extremely difficult to make and have an inconveniently short free spectral range.[2] The first application of echelles was in astronomy. Later came commercial atomic spectrographs. Harrison's work with ruling engines[1] was largely motivated by his desire to rule perfect echelles, an often frustrating task because every success was quickly followed by demands for still greater performance.

Echelles are defined as coarse but precisely ruled gratings that are used only at high angles of diffraction and in high spectral orders. Typical groove frequencies are 316 grooves/mm or fewer, with 20 grooves/mm as a rough lower limit. Angles of incidence vary from 63° to 78° but have occasionally been found as low as 34°. Rarely are spectral orders below 10 used, and the upper limit may vary to as high as 500, although 100 is more common. Because of the high order number and the steep angle of diffraction, they have high dispersion, typically an order larger than standard gratings. Unique to echelles is that they are never used far from the blazed direction, and consequently their efficiency remains relatively high over a large spectral interval. Finally, the higher orders are nearly free of polarization effects. The penalties that must be accepted for so many advantages are that multiple orders overlap and that efficiency varies cyclically within an order.

For historical reasons, echelles are usually ruled with groove frequencies, e.g., 316, 79, 54, 31.6 grooves/mm, although exceptions are quite common. Another prejudice that comes from the old days is to categorize the echelles by their *r* numbers, e.g., *r*-2, -3, -4, which are defined as tangents of the facet angle.

If we examine the pool of experimental and theoretical studies devoted to echelle properties, it turns out to be amazingly shallow. There is no systematic study, the measurements having been performed either with nonlaser light sources[3–5] or on an echelle that was included in some other device.[5–10] The measurements usually cover only a single grating at few wavelength values. The first and probably the

E. Loewen is with Milton Roy Company, 820 Linden Avenue, Rochester, New York 14625; D. Maystre is with the Laboratoire Electromagnetique, Faculté des Sciences et Techniques de Saint Jerome, Avenue Escadrille Normandie–Niemen, 13397 Marseille, Cedex 20, France; and E. Popov and L. Tsonev are with the Institute of Solid State Physics, 72 Tzarigradsko Chausee Boulevard, Sofia 1784, Bulgaria.

Received 24 June 1994.
0003-6935/95/101707-21$06.00/0.

most important reason for a lack of exact knowledge of echelle efficiency behavior is the lack of a superlaser with which to conduct tests. The usual nonlaser sources[3–5] do not have the required monochromaticity (spectral purity) and collimation that are required for accurate determination of the echelle response in high orders. Although common dye lasers have the desirable tunability, they also have a spectral width that is rarely less than 1 nm, so that precise measurements of a maximum whose width is less than, say, 10 nm are almost impossible. Dye lasers are not available in the most interesting region, which is below 400 nm, let alone below 100 nm. That is why most of the deviations from the scalar response of echelles have for a long time either been ignored, blamed on experimental error, or attributed to defective groove geometry.

The second reason for the lack of knowledge of echelles is the lack of a proper theory. The scalar approach is useful[3,4,11–14] until it becomes necessary to investigate deviations from it. Many attempts including shadowing effects have resulted only in inconsistent formulas (higher-order corrections to the simple scalar equations) that are rarely valid even in the limit of their own assumptions. This failure is due to the fact that most of the deviations from the scalar expectations are due to electromagnetic effects, rather than geometrical deficiencies. Although an echelle period can be 10–500 times the wavelength, the small active facet is much shorter than the period. High incident and diffracted angles also complicate the analysis. In some cases, as shown later, cut-off effects (i.e., when the higher orders are passed off) play a significant role, and they cannot be taken into account unless an electromagnetic approach is used—as was shown for echelettes almost a century ago by Lord Rayleigh.[15] Although the electromagnetic theory of gratings has been extensively developed since Rayleigh, especially during the past 25 years,[16] it was difficult to apply to echelles: too many diffraction orders must be taken into account and the profile has edges. The latter condition requires a large number (probably thousands) of Fourier harmonics of the profile function and, when combined with the great number of propagating diffraction orders, gives rise to severe numerical problems. Among them is a requirement to deal with dense matrices of the order of 200, 500, 1000, or even 2000.

Recently Maystre[17] was able to extend the validity of the well-known integral method to the extreme case of echelles with several hundred orders. Precise elimination of the singularities of the kernel of the integral equation was not enough. To account for the specific echelle profile, Maystre carried out the integration along the profile so that the latter was not represented in Fourier series. Special attention was paid to the edges of the profile.

Previous investigations outline two main problems in understanding echelle properties: First, the maximum efficiency is obtained at a wavelength that is slightly shifted from the expected scalar value.[13,18,19] Second, some authors[3,4,13] measure or predict asymmetry of the angular dependence of efficiency with respect to a Littrow mount, whereas others[11] confirm such symmetry.

If we try to summarize the deviations from scalar echelle behavior, two main groups of effects can be distinguished:

(1) Theoretical deviations, which include

- a shift in the maximum position between TE and TM polarizations, even for perfectly conducting substrates,
- finite-conductivity effects, and
- cut-off effects that are due to the echelle passing off the higher orders.

(2) Technological and experimental problems, which include

- deviation from the desired facet angle,
- profile deformations (deviations from the plane facet),
- finite-beam effects, and
- influence of surface roughness.

In what follows we analyze the spectral and angular behaviors of echelles and compare them with scalar expectations. Although the latter are not precisely defined, we try to specify them in each case. Finite-beam effects and surface roughness are beyond the scope of this paper, although they can lead to some measurable deviations from symmetry with respect to a Littrow mount. The investigation includes several different echelles with 316, 79, and 31.6 grooves/mm and two typical facet angles: 64° and 76°. Spectral and angular measurements were performed on a single echelle that was not included in another device. In all cases laser sources were used. The data are compared with the numerical results on the basis of rigorous electromagnetic theory, and when necessary the theory has been used to give more precise and detailed information to facilitate understanding. For this paper we made almost all the experimental measurements at a constant wavelength and with variable angles of incidence. It is not only easier but also provides better insight. By numerical means either approach can be simulated.

2. Blazing—the Spectral Response of Echelles

The behavior of echelles is discussed in many optics textbooks. For clarity, we briefly summarize the most common approaches to the blazing phenomena. As usual, θ_i is the illuminating angle, d is the grating period, θ_d is the angle of diffraction, and λ is the wavelength. It is necessary to give some definitions for the terms used further on, because there is no commonly accepted opinion in the literature. At first, the term blazing is taken to mean the set of conditions for which maximum efficiency is observed in a given order. The blazing in one order is perfect

when, at the peak, no light is scattered into any of the other orders. Blazing can occur when different parameters are varied, namely, the angle of incidence and the wavelength. Their values, which correspond to the blazing, are called the blaze wavelength λ_B and the blaze angle of incidence θ_B. To distinguish between the local maxima of efficiency [see Fig. 9(a)] and the blazing (maximum maximory), these local maxima are called just maxima, and the corresponding angles are called angles of maximum efficiency, and not blaze angles.

According to scalar theory, perfect blazing occurs when the angle of incidence is equal to the facet angle and the wavelength is given by Eq. (3) below. We call these values the ideal blaze angle and the ideal wavelength, respectively, to distinguish them from the real ones, which appear to be slightly shifted from the ideal.

Sometimes the facet angle ϕ_B is also called the blaze angle, because of its equality in scalar-optics approaches. We try to avoid this. However, to make a proper connection with scalar-theory expectations, we talk about the observed-apparent facet angle $\tilde{\phi}_B$ that is obtained from the real blaze wavelength, which is introduced into Eq. (3). It differs from the real facet angle because of the electromagnetic character of light scattering. Manufactured echelles are usually characterized by their nominal facet (blaze) angle—the facet angle that is supposed to have been ruled—and it always differs somewhat from the real one.

We also call some of the orders blaze, referring to their high efficiency for a given wavelength in comparison with the others. The blaze-order number, of course, changes with the wavelength.

2.A. Kirchhoff Approach

The Kirchhoff diffraction theory in the Fraunhofer approximation expresses the grating's scattering of incident light as a product of two terms, the interference function I_f and the intensity function of a single slit, also called the blaze function, B_f, so that the normalized intensity function of a grating that consists of M identical slits I_g is given by

$$\frac{1}{M^2} I_g(p) \equiv I_f B_f = \left[\frac{\sin\left(M \frac{kdp}{2}\right)}{M \sin\left(\frac{kdp}{2}\right)}\right]^2 \left[\frac{\sin\left(\frac{ksp}{2}\right)}{\frac{ksp}{2}}\right]^2, \qquad (1)$$

where the first term represents the normalized interference function, the second term represents the slit-intensity function, s denotes the slit width, and $p = \sin\theta_d + \sin\theta_i$. The interference function I_f has maxima when $p = N\lambda/d$, i.e., in directions that are given by the grating equation. Between them there are weak secondary maxima. For large values of M (the number of the illuminated grooves) the secondary maxima are weak. They are separated by points of zero intensity in directions given by

$$p \equiv \sin\theta_d + \sin\theta_i = \frac{N}{M}\frac{\lambda}{d}. \qquad (2)$$

The slit-intensity function depends on the form of the grooves. It has a maximum in some direction, called the blazed direction or the blazed wavelength, if it is considered to be a function of the wavelength. Compared with the interference function with large values of M, the slit-intensity (groove) function falls off slowly on both sides of its maximum, so that the grating response (the intensity function of the grating) consists of sharp peaks (determined by I_f), which are modulated by the slit-intensity function.[20] When the Kirchhoff approximation is applied to a set of parallel slits,[20] the blaze function has a prime maximum when the angle of diffraction is equal to the angle of incidence and both are measured with respect to the slit normal.

2.B. Mirror-Reflection Approach

Blazed gratings are expected to respond, over a certain wavelength and angular interval, like perfect mirrors that are equipped with angular dispersion: They are supposed to diffract the entire incident light into a given order, under given incidence conditions. These expectations come from the simplest geometric approach, according to which the strongest diffraction (blazing) occurs when an order is diffracted by a grating (with a profile consisting of a simple right triangle) in a direction as if it were being reflected by a large (or small, in the case of echelles) facet. If the facet is characterized by an angle ϕ_B (see Figs. 1) and if the incident wave illuminates the grating surface under the same angle (with respect to the grating normal), the necessary condition for an order with a number, namely, $-N$, to be diffracted backward is given by the simple equation

$$2\sin\phi_B = -N\frac{\lambda}{d}, \qquad (3)$$

and taking into account the grating equation this becomes

$$\sin\theta_N = \sin\theta_i + N\frac{\lambda}{d}, \qquad (4)$$

where the minus sign before N in Eq. (3) responds to the fact that for positive angles of incidence blazing occurs in negative orders, so that the order-numbering convention is opposite the one usually used in grating studies. This is convenient, because it is not always necessary to carry the negative sign of the order number. There will be no confusion, because there is high asymmetry in the number of propagating orders, which is due to the high angle of incidence and the small wavelength-to-period ratio.

2.C. Wave-Optics Approach

The intuitive reflection arguments have a stronger background in wave optics. Suppose that the inci-

dent wave and the scattered wave have opposite directions of propagation that are perpendicular to the facet. The optical path difference D_{opt} of the waves, which are scattered on two neighboring facets, should be equal to twice the length of the second facet. Then Eq. (3) would immediately indicate that D_{opt} is an integer times the wavelength, i.e., the scattered waves interfere constructively, so that blazing occurs.

2.D. Rigorous Electromagnetic Approach

It is surprising to find that there are cases when the considerations described above, which are valid in the geometrical-optics approximation, are also rigorous from an electromagnetic point of view, i.e., whenever the groove dimensions are comparable to wavelength. Then we arrive at the well-known theorem developed by Marechal and Stroke[21] for determining perfect blazing in TM-polarized light that is diffracted by a perfectly conducting echelette grating. This theorem (Theorem 1) states that perfect blazing occurs when the angle of diffraction is equal to the angle of incidence, which in turn is equal to the facet angle, provided that the apex angle is 90° (we assume that the material is perfectly conducting) and provided that the light is TM (or *S* or *p*) polarized, with the magnetic-field vector being parallel to the grooves. There is a simple proof for the theorem, so simple that it is worth repeating.

Perfect conductivity requires that the tangential electric field be zero on the grating surface. Let us assume that, above the grating surface (including the region inside the grooves), there are only two plane waves, the incident and the diffracted, and both are perpendicular to one of the facets (namely, *A* in Figs. 1). Their magnetic-field vector is parallel to both *A* and *B*, and the electric-field vector is parallel to *A* and perpendicular to *B*. The latter fact automatically ensures that along the second facet (*B*) the tangential electric field is zero. Then if the amplitudes are equal but opposite in sign, the total electric-field vector (sum of the two terms) is zero on *A*, i.e., the boundary conditions are fulfilled. The two plane waves are solutions of the Maxwell equations and of the outgoing-wave conditions. The uniqueness of the solution of the scattering problem leads to the conclusion that all the incident light is diffracted backward.

Rigorous numerical calculations[20] have already proved the validity of the theorem of Marechal and Stroke, from order -1 to very high orders, as high as possible (as of now the limit exceeds 600, as shown later). An example of the expected spectral response of a blazed grating is presented in Fig. 2. The angle of incidence is kept constant and equal to the facet angle. With a wavelength increase and at given values, orders with consecutive numbers obey Eq. (3), the light is diffracted completely into each order, and all the others are equal to zero. The distance between two consecutive maxima can be easily derived from Eq. (3) and is proportional to λ^2.

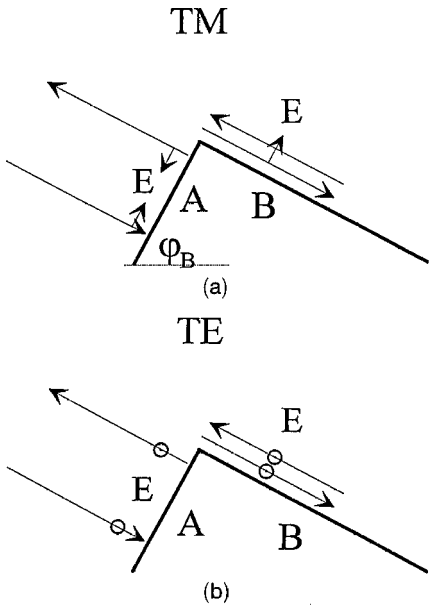

Fig. 1. Schematic representation of the wave vectors and electric-field vectors of incident and diffracted-backward plane waves along the two facets of a triangular grating with a 90° apex angle. The two planes of polarization are TM and TE. E represents the electric field; the open circles indicate that the direction of the field is perpendicular to the paper in the TE case, and the circles with center dots represent that there is no center within these circles.

2.E. Real Blazing Problem

Unfortunately, life is not always easy and simple. For decades both manufacturers and users have noticed that gratings exhibit a behavior that fails to obey intuition fully. It has been a long-held belief that echelles with periods of 20 or even 50 wavelengths long should have a good response that is predictable by simple scalar (nonelectromagnetic)

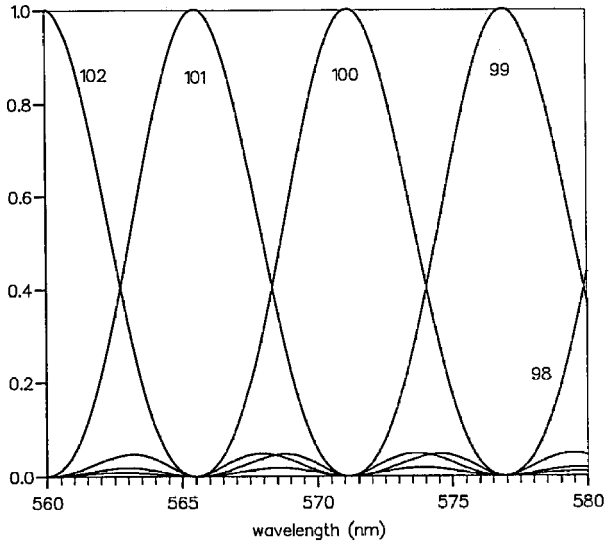

Fig. 2. Numerical results showing the spectral dependence of the diffraction efficiency in the TM plane of a perfectly conducting *r*-2 echelle with a 90° apex angle and 31.6 grooves/mm. The angle of incidence θ_i is equal to the facet angle ϕ_B, which is equal to 64.48°. The vertical axis is the efficiency.

theories. However, it was during accurate measurements that the real blaze wavelength and the real blaze angle were found to be slightly shifted from those predicted by Eq. (1).[13,18,19] The trivial conclusion that the facet angle is different from the one specified by the manufacturer may be assumed to be true, but it does not explain why this shift varies with the wavelength, e.g., decreases for shorter waves. A guide to understanding (or at least accepting) this deviation can be found if we return to the proof of Theorem 1. This proof does *not* hold for TE polarization, even if we have a perfectly conducting echelle. Whereas the boundary conditions along the active facet *A* can again be satisfied by only two waves that are perpendicular to this facet, the electric-field vector, which is parallel to the grooves for this polarization, is parallel to the other facet *B*, so that the two waves alone that satisfy the boundary conditions for *A* cannot satisfy the boundary conditions along the entire grating surface.

In fact both experiment and theory show in a determined manner that the TE case differs more or less from that of TM (see Figs. 3). One might expect that the difference in the high orders is small enough to be neglected. However, with the maximum width decreasing according to λ^2, even a small shift Δ_λ of the maximum position can, and certainly does, lead to measurable effects. Electromagnetic theory, and in particular the only available numerical code that can serve to analyze echelle behaviors, is able in principle to act as a numerical superlaser, effectively supplying us with a monochromatic, collimated beam with precision to the 15th digit, as well as with the same precision in tuning accuracy. This is sufficient, at least if we limit ourselves to, say, the 1000th order; of course, the precision is much higher than what is experimentally available. The usual checks, including convergence and energy balance (for a perfectly conducting substrate), were used, and a check against the experimental observations was also done whenever possible (see Subsection 2.F).

2.F. Numerical Results

Investigation of several different echelles reveals some common features. First, we found that numerical results show perfect blazing in the TM case for a perfectly conducting substrate to be in the position predicted by Theorem 1, when started from the first order and continuing to the 660th order, which is a severe test of the code. We stopped at the 660th order mainly because of calculation-time problems. Second, even for the perfectly conducting case, TE blazing shifts to a shorter wavelength [see Fig. 3(a)], and blazing can never be perfect except with a grating that supports only two propagating orders. This condition can happen only in an echelette grating, never in an echelle. Third, a finite but highly conducting substrate does not significantly change the TE response; it merely introduces a reduction factor to account for the reduced reflectivity. The TM efficiency is reduced more significantly, and the position of its maximum is shifted toward the TE maximum, with the exact behavior depending on the substrate index. A typical example is shown in Fig. 3(a).

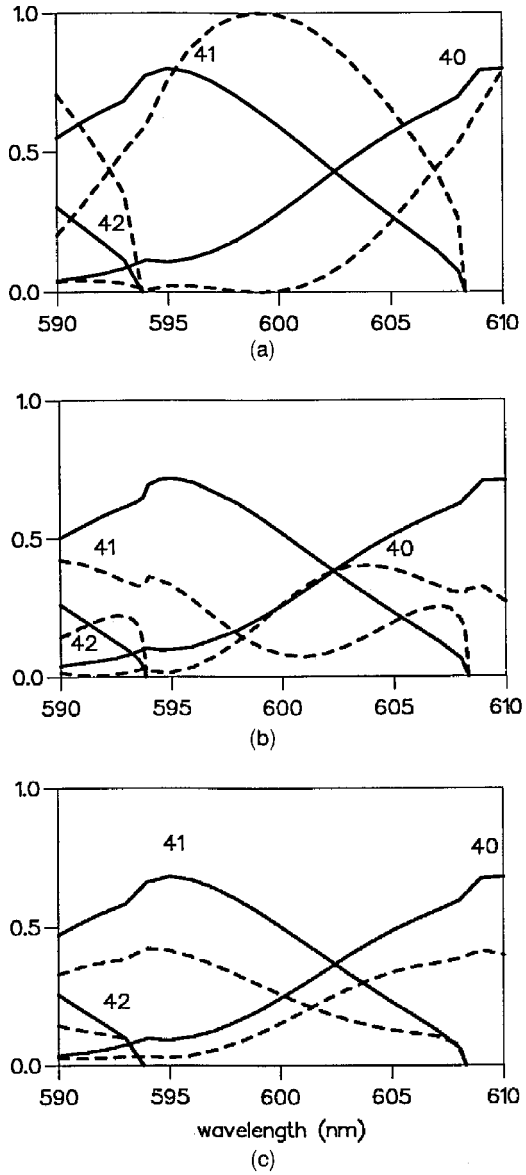

Fig. 3. Numerical results showing the spectral dependence of the diffraction efficiency of an *r*-4 echelle with 79 grooves/mm. $\theta_i = \phi_B = 76°$. The solid curves represent the TE case, and the dashed curves represent the TM case for (a) a perfectly conducting substrate, (b) $n\text{Al} = 1.2 + i7$, (c) $n\text{Al} = 1.09 + i5.31$. The vertical axes are in arbitrary units.

With a decrease in the λ/d ratio, the positions of the consecutive maxima are given from the theorem of Marechal and Stroke:

$$\lambda_{B_N} \propto \frac{1}{N}. \tag{5}$$

This proportion is rigorously fulfilled in the TM case for a perfectly conducting substrate when the ideal and the real blaze wavelengths coincide. It is only

approximately valid for the real blaze wavelength for all other cases. The separation between two consecutive maxima and the half-width of each maximum is proportional to N^{-2} for high N:

$$\lambda_{B_N} - \lambda_{B_{N+1}} \propto \frac{1}{N} - \frac{1}{N+1} \approx \frac{1}{N^2}. \tag{6}$$

At shorter wavelengths, the difference between the TE and TM cases decreases so that the spectral response becomes less polarization dependent. Figures 4 illustrate the spectral responses in the two fundamental polarizations for an echelle with 79 grooves/mm and a 76° facet angle (r-2). The angle of incidence is kept equal to the facet angle. The substrate is aluminum. The maxima values increase slowly with the order N, and the positions of the maxima become closer to the position predicted by blazing Eq. (3). The spectral dependence of the shift Δ_λ of the maximum is plotted in Figs. 5 for several different echelles. It is astonishing to find a well-defined power dependence, which is

$$\Delta_{\max_N} \propto \frac{1}{N^{2+\delta}}. \tag{7}$$

For r-2 echelles, $\delta = 0.6$. For r-4 echelles, δ has the same approximate value, 0.6, when $N > 65$, but $\delta = 0$ when $N < 65$. A similar rule holds for another echelle (44 grooves/mm and a facet angle of 70°), for which the analysis includes blazing in very high orders (to 660; see Fig. 6). If perfect conductivity is assumed so as to suppress the decrease of aluminum's reflectivity below 50–100 nm, the maximum shift of the TE case from the position of the TM maximum is also given by relation (7), with $\delta = 0.6$ (squares in Figs. 5). A smaller facet (and thus blaze) angle leads to a smaller shift [compare the circles and crosses in Fig. 5(b) with the squares, triangles, and diamonds].

Although it is nontrivial, this rule [relation (7)] has a straightforward physical interpretation. It shows that, when the wavelength-to-period ratio decreases, for positive δ the difference in the positions between the TE and TM spectral curves for each order reduces faster than the separation between the consecutive orders (which is proportional to N^{-2}). This behavior corresponds to the most natural scalar expectations that, for $\lambda \to 0$, not only the positions of the maxima but also the positions of the curves for the TE and TM cases for any order would merge into each other. Otherwise, for negative δ, the maxima would approach each other, but their relative separation would increase, as given by

$$\frac{\lambda_{B_N}{}^{\mathrm{TE}} - \lambda_{B_N}{}^{\mathrm{TM}}}{\lambda_{B_N}{}^{\mathrm{TM}} - \lambda_{B_{N+1}}{}^{\mathrm{TM}}} = \frac{1}{N^\delta} \xrightarrow[\lambda \to 0]{} \begin{cases} \infty & \delta < 0. \\ 0 & \delta > 0 \end{cases} \tag{8}$$

In fact, Figs. 5 are a direct demonstration that in the scalar limit ($\lambda/d \to 0$) the echelle behavior becomes more scalar, i.e., the difference between the TE- and TM-polarization responses decreases. Until now, we knew that in and close to the resonance domain the polarization effects were strong, and we believed that in the scalar domain these effects disappeared, but the results shown in Figs. 5 prove that these conclusions are true and demonstrate how they happen.

The abrupt change in the behavior of the r-4 echelle (Figs. 4 and 5) below $N = 65$ is due to cut-off effects. For shorter wavelengths both the -1 and $N + 1$

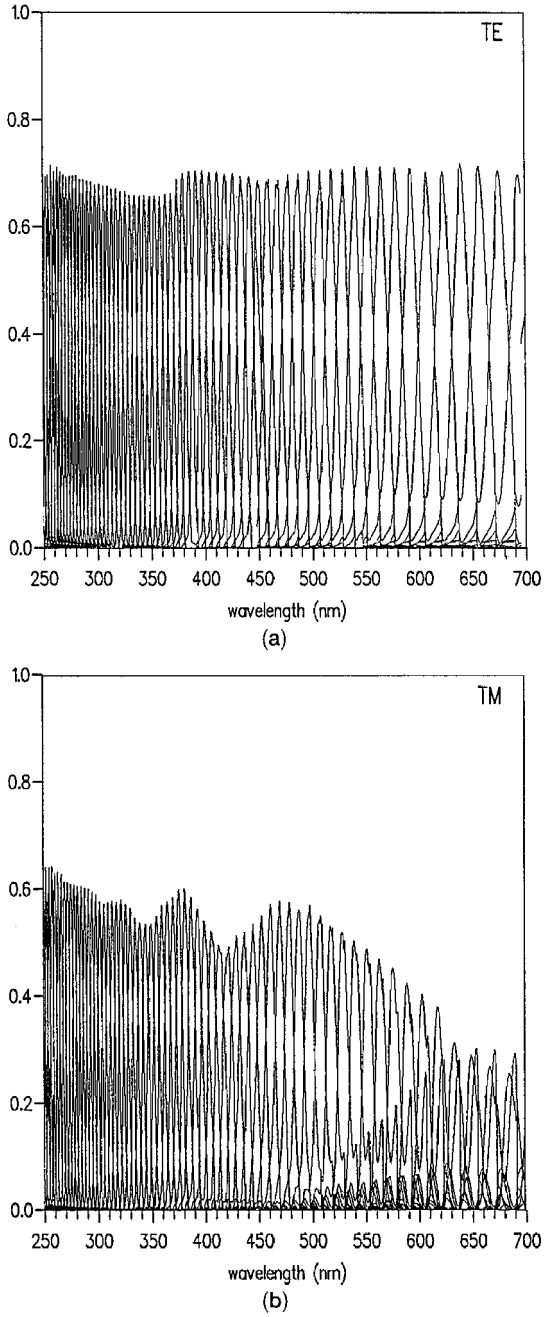

Fig. 4. Numerical results showing the spectral dependence of a large spectral interval on the diffraction efficiency of an r-4 echelle with 79 grooves/mm. $\theta_i = \phi_B = 76°$. The refractive index corresponds to the bulk values of aluminum, and its dispersion is taken into account. (a) TE and (b) TM polarization. The vertical axes are in arbitrary units.

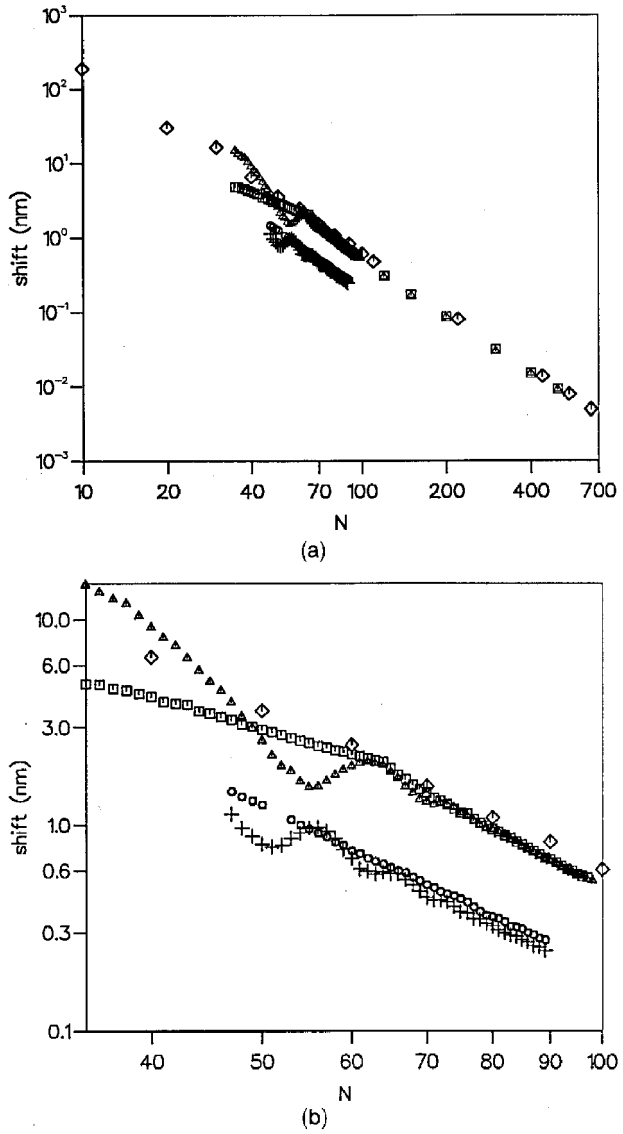

Fig. 5. Numerical results showing the spectral shift of the position of the maximum from the scalar position given by Eq. (3). A double-logarithmic scale is used. Squares represent an *r*-4 aluminum echelle with 79 grooves/mm and TE polarization; triangles represent the same but for the TM plane. Circles and crosses represent the TE- and TM-plane results, respectively, for an *r*-2 aluminum echelle with 79 grooves/mm. Diamonds represent the TE case for a perfectly conducting echelle with 43 grooves/mm and a 70° facet angle. The central part of (a) is shown enlarged in (b).

orders propagate (N denotes the blazing order), and for longer waves they are cut off so that the blaze order is the last one that can diffract. The cutoffs can also be detected in the spectral dependence (see Fig. 7), and the cutoff closest to the blaze order has the greatest influence. That is why these effects play a negligible role for echelles with smaller facet angles or a higher number of blaze orders, when there are several propagating orders of a higher number than that of the blaze order (e.g., an *r*-2 echelle).

The role of cut-off effects is much stronger in the angular dependence of efficiencies, as is well known

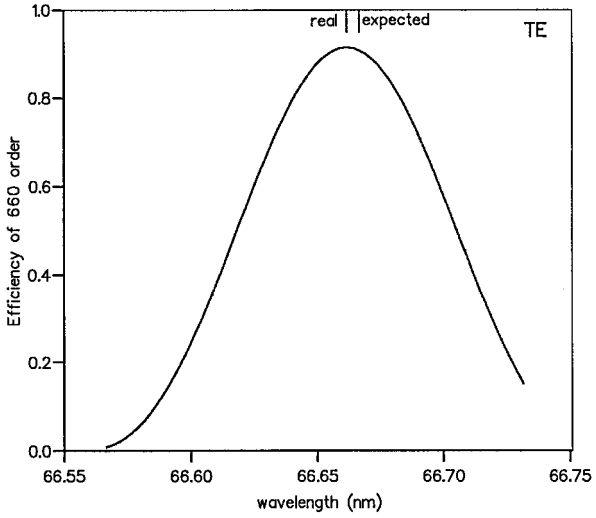

Fig. 6. Record of numerical investigation: Efficiency in order 660 for the TE case with a perfectly conducting echelle with 42.713 grooves/mm. $\theta_i = \phi_B = 70°$. The position of the maximum (labeled real) is shifted from the ideal position (labeled expected) as determined from Eq. (3).

for echelettes. However, this is the first investigation to demonstrate that these effects can also exist for echelles. To complete this picture, the results of the spectral measurements of efficiency of an *r*-4 echelle with 79 grooves/mm are presented in Figs. 8 (solid curves represent TE and dashed curves TM polarization). A standard dye laser pumped by a 15-W Ar^+ gas laser was used, and the results show typical behavior. We present them to illustrate the difficulties in making spectral measurements, and, in particular, the difficulty in the precise determination of the spectral shift of the maximum. The shift rapidly decreases with the wavelength, and below 300 nm it can become less than 1 nm, or even less than 0.1 nm. Moreover, near the maximum, the maximal value depends weakly on slight changes of the incident and facet angles, so that when the latter is not known (and it never is), the true position of the maximum can hardly be found with enough precision to determine its shift, whereas there is no such difficulty regarding the numerical results [Fig. 8(b)].

3. Angular Response of Echelles

It is well known among grating theoreticians, manufacturers, and users that when one (namely, the nth) diffracted order propagates backward it is called the nth-order Littrow mount. It is defined by an equation similar to Eq. (3):

$$2 \sin \theta_i = -n \frac{\lambda}{d}. \tag{9}$$

There is another important theorem that is valid no matter what the grating material, period, groove shape, groove depth, incident-wave polarization, or diffraction-order number. This is Theorem 2, which states that the efficiency and the phase in a given diffracted order are symmetrical with respect to the

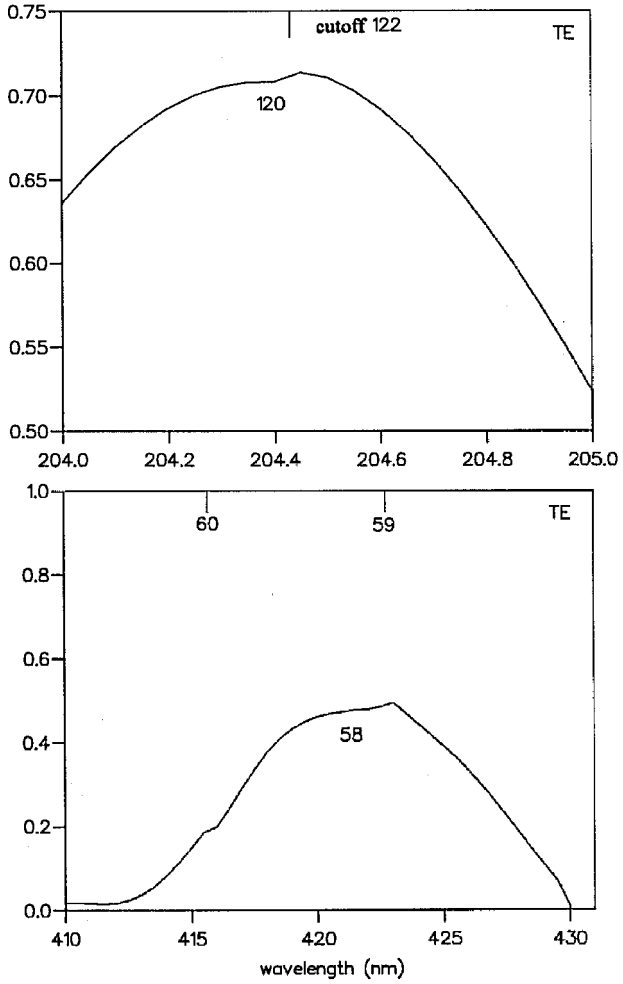

Fig. 7. Numerical results showing the TE efficiency in orders 120 and 58 for the TE plane of an *r*-4 echelle with 79 grooves/mm. $\theta_i = \phi_B = 76°$. The passing-off positions of the adjacent orders are indicated at the tops of the graphs. Note the magnification of the ordinate for order 120, which was necessary to reveal the cut-off anomaly.

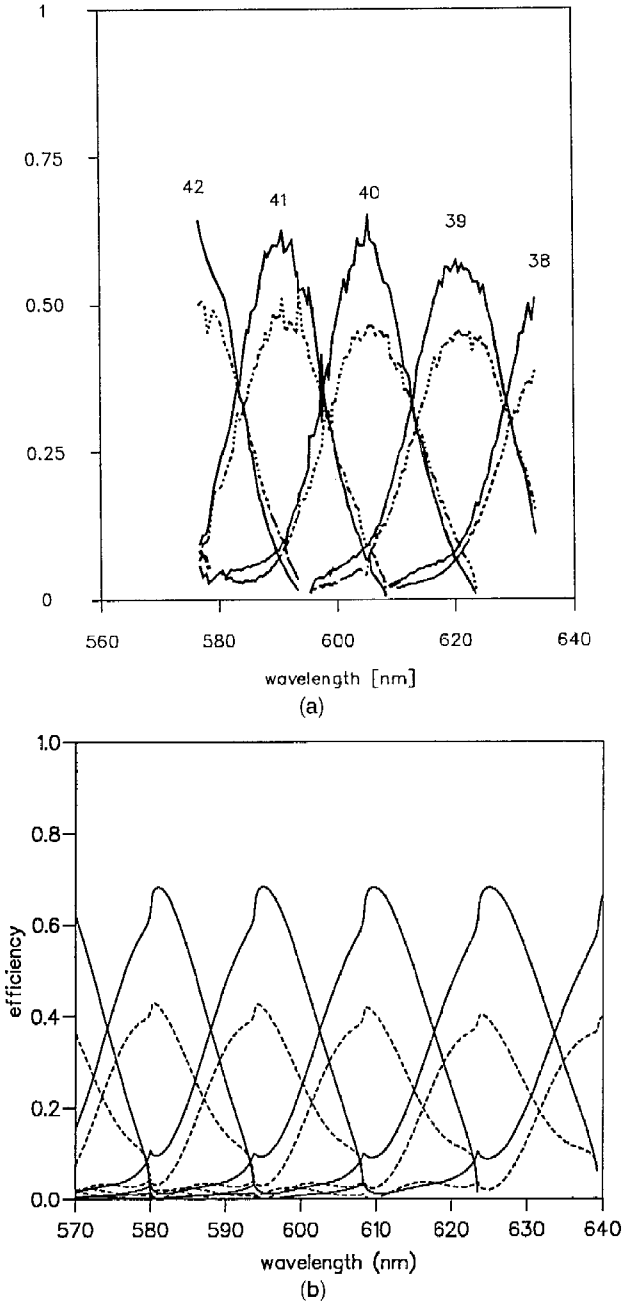

Fig. 8. Dye-laser measurements of (a) the diffraction efficiency in several consecutive orders for an *r*-4 echelle with 79 grooves/mm, where $\theta_i = \phi_B = 76°$, and (b) the corresponding numerical results with $n_{A1} = 1.9 + i5.31$. The vertical axes are in arbitrary units.

angle corresponding to its own Littrow mount, and the symmetry concerns the dependence of the sine of the angle of incidence. It is interesting to note that it is only in the case of diffraction by echelles that the validity of this theorem has been questioned[3,4,13]; in all other grating applications and theories it has been taken as something quite basic.

Of course, the theorem can be clearly understood only for the ideal case of perfect periodicity and a plane-incident wave. Otherwise, e.g., with high random roughness or a narrow incident beam, slight differences can be observed at the two sides of the Littrow mount in the angular dependence of the diffraction efficiency.

The most important question from a practical point of view is how the departure from a Littrow mount affects the efficiency (the blazing), because in real devices gratings are almost never used under perfect autocollimation conditions. Let us recall a geometrical-optics formulation of the blazing conditions. The maximum in a given order occurs when light is diffracted by the grating as if being reflected by the small facet. When the incident wave is perpendicular to this facet, this condition requires a Littrow mount and corresponds to ideal blazing. But the reflection can be performed at a different incident direction. Let us denote with Δ_θ the angle between the incident beam and the direction normal to the facet. The reflection conditions require that the angle of diffraction with respect to the facet normal be equal to Δ_θ, i.e.,

$$\theta_N = \phi_B - \Delta_\theta, \tag{10}$$

when

$$\theta_i = \phi_B + \Delta_\theta. \tag{11}$$

Simple calculations with Eqs. (3) and (4) show that for each Δ_θ a maximum can be expected at a wavelength λ_Δ such that

$$\cos \Delta_\theta = \frac{\lambda_\Delta}{\lambda_B}. \tag{12}$$

The opposite conclusion is also true: Whenever maximum efficiency is required at a wavelength slightly different from the blazed one, the addition of a small angular deviation can serve as a solution. However, because of the cosine term in Eq. (12), this is possible only if $\lambda_\theta \leq \lambda_B$. Figure 9 illustrates this rule. For wavelengths smaller than the blaze wavelength, two lateral maxima are observed, and their separation $2\Delta_\theta$ is given quite well by Eq. (12). For longer wavelengths there is a single maximum located at the corresponding Littrow angle. The maximum decreases with its departure from the blaze wavelength. It must be pointed out that because of the relatively high incident and diffracted angles, the angular dependencies appear to be asymmetrical with respect to the Littrow mount. True symmetry exists when the abscissa is represented in terms of $\sin(\theta_i)$, rather than in terms of θ_i.

Equation (12) also has an unexpected but important role in the determination of the facet angle. It is well known that, when one performs ruling and replication, the facet angle is rarely found to be exactly what was desired. Sometimes a departure of 0.1° can be critical. Of course, one usually compensates by tuning the angle of incidence so that maximum efficiency is obtained under the desired conditions. Using Eq. (12) we can determine the ideal blaze wavelength from angular, rather than spectral measurements, which is an advantage because the former is more precise and easier to handle.

In the following sections we give experimental data for five different echelles. The choice starts with echelles that work in high orders and exhibit an almost scalar behavior, with 31.6 grooves/mm and two nominal facet angles: 63.5° and 76°. In fact, numerical fitting shows that the real facet angle of the first sample is close to 64.5°. The second set consists of two echelles (*r*-2 and *r*-4) with 79 grooves/mm. The *r*-4 echelle exhibits effects that are strange and unexpected for echelles, but typical for gratings with smaller periods. These are the so-called cut-off effects that are due to the orders next to the blaze order having passed off. The third example has 316 grooves/mm, and its efficiency is strongly influenced by polarization.

Theoretical confirmation is presented only for the most interesting cases because of the lack of space. Coincidence between theory and experiment is always of the same order as in the cases presented: The general features of the efficiency behavior are the same, differences exist mainly in the maximum values.

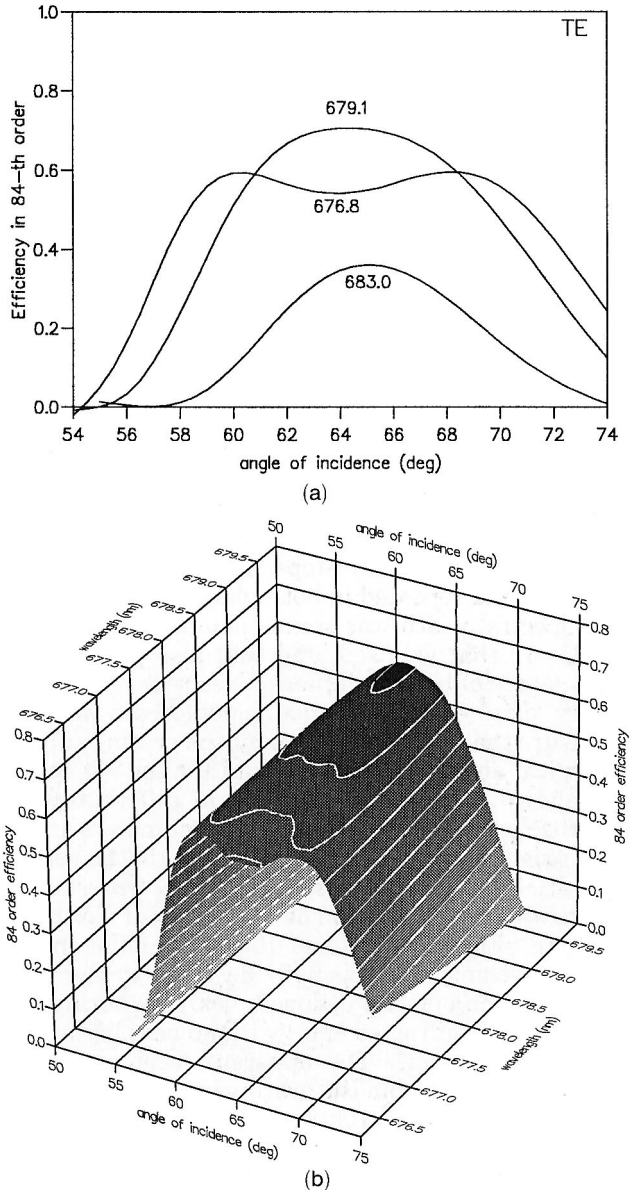

Fig. 9. Numerically determined efficiency of the 84th order for an *r*-2 echelle with 31.6 grooves/mm and a 64.48° facet angle. (a) The angular dependence for several wavelength values, shown in nanometers in the figures. (b) A three-dimensional view of the efficiency peak in the wavelength and the angle of incidence planes.

These differences can be easily explained by the deviations between ideal gratings and real ones, as discussed in detail in Section 4. Lower-order echelles exhibit higher values of theoretical polarization dependence, and the difference decreases with an increase in order, which can also be explained by the deviations between the real and ideal grating parameters. A typical example is the decrease in polarization effects [Figs. 3(b) and 3(c)] when the assumed refractive index is changed.

A common feature, which is a direct consequence of Theorem 2, has to be pointed out regarding all the efficiency curves. The efficiencies of all the orders are a symmetrical function of the sine of the angle of incidence with respect to each orders own Littrow

mount. Thus, an observed asymmetry with respect to the facet angle is not strange. It is due to two reasons: First, for wavelengths differing from the ideal blaze values, the Littrow mount does not coincide with the facet angle. Second, at high incident angles the symmetry in sine differs from the symmetry in the angle of incidence. However, in all the cases that we observed, deviations from Theorem 2 never exceeded the experimental error.

3.A. Efficiency Behavior in High Orders

To examine high-order behavior, use was made of 31.6-groove/mm echelles at two different and frequently used groove angles of 63.5° (*r*-2) and 76° (*r*-4), over a wavelength range of 441.6–676.4 nm, which corresponds to orders from 84 to 139. The range was determined by the set of available lasers: He–Cd, Ar^+, He–Ne, and Kr^+. In each case data were taken in small angular steps, so as not to miss any features, and repeated in both planes of polarization. The spectral width was small enough, thanks to the gas lasers that we used, and that also provided the high degree of beam collimation desired. When necessary, diaphragming of the incident beam was used to ensure that the entire beam hit the grating surface.

Typical absolute efficiency data for the *r*-4 echelle are shown in Figs. 10 for several different wavelengths, which are indicated in nanometers in the upper right-hand corners (in Figs. 10–15, the vertical axes are in arbitrary units, solid curves represent TE polarization, and dashed curves represent TM polarization). Figures 10(a) and 10(i) are similar in that their wavelengths happen to lie close to the blaze values, which one can deduce quickly by noting that there is little diffracted energy in the next higher and next lower orders. The apparent facet angle that can be evaluated from the grating equation is close to 75.9°. In both Figs. 10(a) and 10(i), the polarization level (the difference of the TE and TM efficiencies divided by their sum) is close to 6%, which seems high for orders near 100.

At 496.5 nm [Fig 10(f)] we find ourselves near the half-order position between orders 123 and 124. A somewhat similar situation can be seen at 676.4 nm [Fig. 10(k)]. The rule established by Eq. (12) can be clearly observed: The angular dependence of the higher order (with the lower blaze wavelength) is characterized by a single maximum that has a lower value than the blaze maximum [compare orders 124 and 91 in Figs. 10(f) and 10(k) with orders 139 and 97 in Figs. 10(a) and 10(i)]. The lower order [the best example is order 123 in Fig. 10(f)] has two maxima separated by an 8.5° angular interval. Using Eq. (12) we can deduce an apparent facet angle of 75.4°. However, this rule cannot be utilized precisely enough for echelles with facet angles as high as this one, because cut-off effects introduce edges in the efficiency curves. The rule works perfectly when we use smaller facet angles, which we show in Figs. 11 with the experimental results and in Figs. 12 with the corresponding theoretical data for an *r*-2 echelle. This echelle has the features that are the closest to scalar ones.

There are several sets of common figures. The central orders at 488.0, 496.5, and 514.5 nm [Figs. 11(e), 11(f), and 11(h), respectively] seem almost identical, and the adjacent orders all have comparatively low efficiencies. However, if we assume that these figures correspond to perfect blazing and try to determine the facet angle by using the grating formula in Eq. (3), the error is too great: Whereas the 117th order [Fig. 11(e)] gives $\phi_B = 64.44°$, which is close to the real value, the 115th order [Fig. 11(f)] results in $\phi_B = 62.5°$, and the 111th order [Fig. 11(h)] shifts ϕ_B to 58.8°, which is much too far from the real value. The conclusion is that the 111th order is not as close to blazing at 514.5 nm as might be concluded from Fig. 11(h). It is much safer to depend on orders that appear to lie below the blaze. Several figures show such wavelength values, and the data are summarized in Table 1. At different wavelengths (column 1) there are several orders of relatively high efficiency with blaze wavelengths higher than the one tested. In this case there are two lateral maxima in the angular dependencies of these orders (column 2), separated by $2\Delta_\theta$ (column 3). Column 4 contains the values of the observed facet angle $\tilde{\phi}_B$, which were obtained from the scalar approach through the use of Eqs. (3) and (12). There are two sets of values—experimental and theoretical. The latter were obtained with the assumption of a facet angle $\phi_B = 64.48°$. It is obvious that the apparent blaze angle varies with λ, even in the theoretical results, which is an indication that this is neither experimental error nor just a deviation of the real facet angle from the nominal. Using relation (8) with $\delta = 0.6$, we have tried to reconstruct the true experimental facet angle from the apparent one. The difference between the true and apparent facet angles for both the theoretical and the experimental data is presented in the last column of the table. Although scattering of the data is high, the tendency for a decreasing value with a decreasing wavelength can be clearly observed.

For comparison, we present the numerical results of the rigorous theory in Figs. 12 with the assumption that the facet angle is equal to 64.48°, a value that we obtained by numerically fitting the experimental curves over the entire spectral interval of the measurements. Coincidence is very good, especially as it concerns the position of the maxima of all the orders. The main difference is observed with respect to the maximum efficiency values of the strong orders for which the theoretical results are always higher. This can be explained in view of the results in Section 4 in that deviations of the real profile from the ideal triangular one with a 90° apex angle invariably leads to a loss of performance. The lower polarization dependence in comparison with the previous *r*-4 echelle is observed in both the experimental and theoretical results.

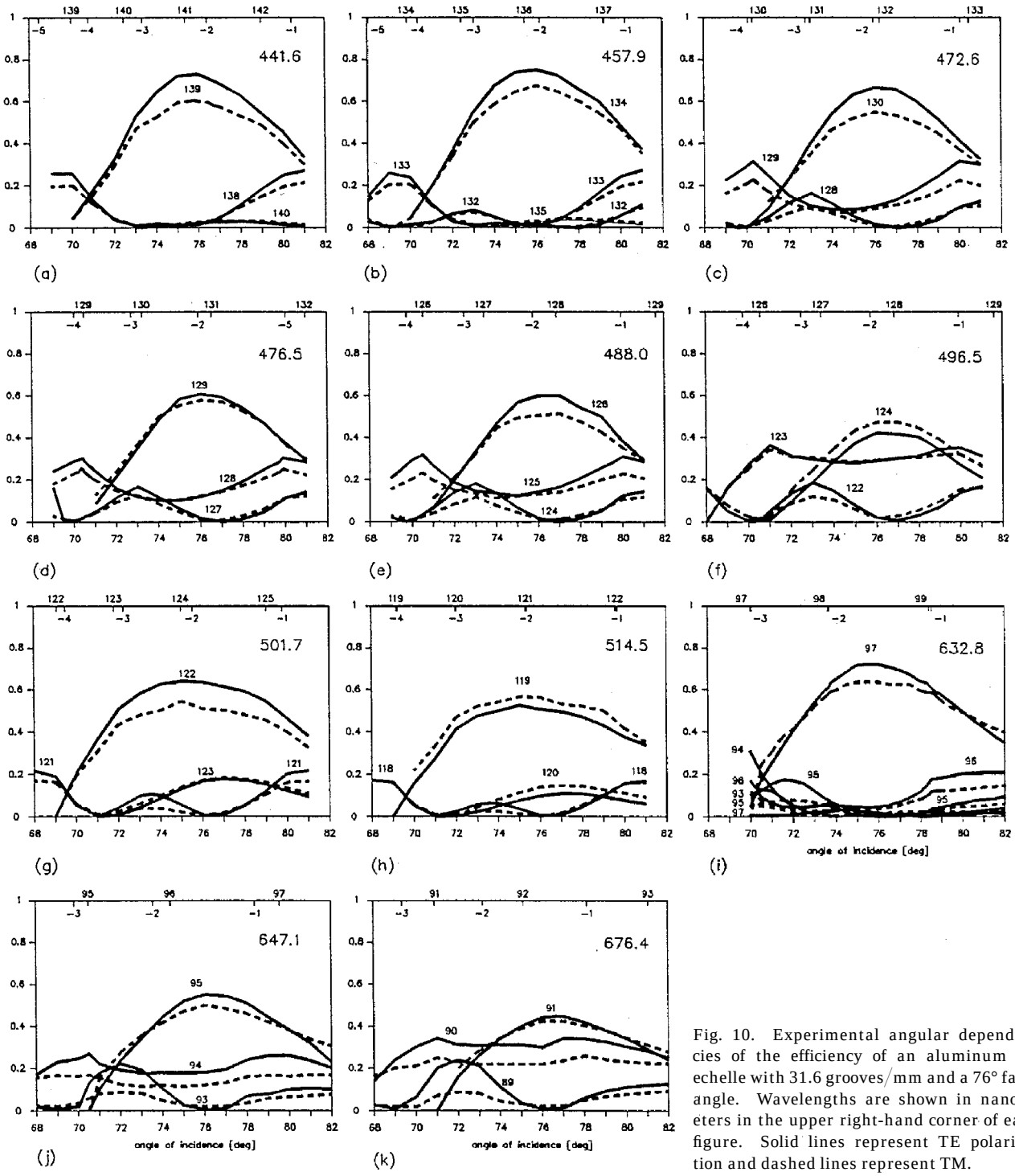

Fig. 10. Experimental angular dependencies of the efficiency of an aluminum *r*-4 echelle with 31.6 grooves/mm and a 76° facet angle. Wavelengths are shown in nanometers in the upper right-hand corner of each figure. Solid lines represent TE polarization and dashed lines represent TM.

3.B. Efficiency Behavior in the Medium Orders: Cut-off Effects

The region with the medium orders is represented by the family of 79-grooves/mm echelles, which is probably the most widely used of all echelle families. The visible portion of the spectrum is covered conveniently by orders from 30 to 60, although these echelles have been used in the UV in orders to as high as 100 or even 180.

Starting with the high-angle (*r*-4) echelle, we present the results in Figs. 13(a)–13(m). Even at the lowest available wavelength, 441.6 nm (see upper right-hand corners of figures for wavelengths), there are peculiarities when compared with the higher-order echelles (Subsection 3.A). We can see an unusual and sharply defined dip in the efficiency right in the center of the blaze peak [Fig. 13(a)]. Similar dips occur at 457.9, 472.6, 476.5, 501.7, 514.5, 596.9, and

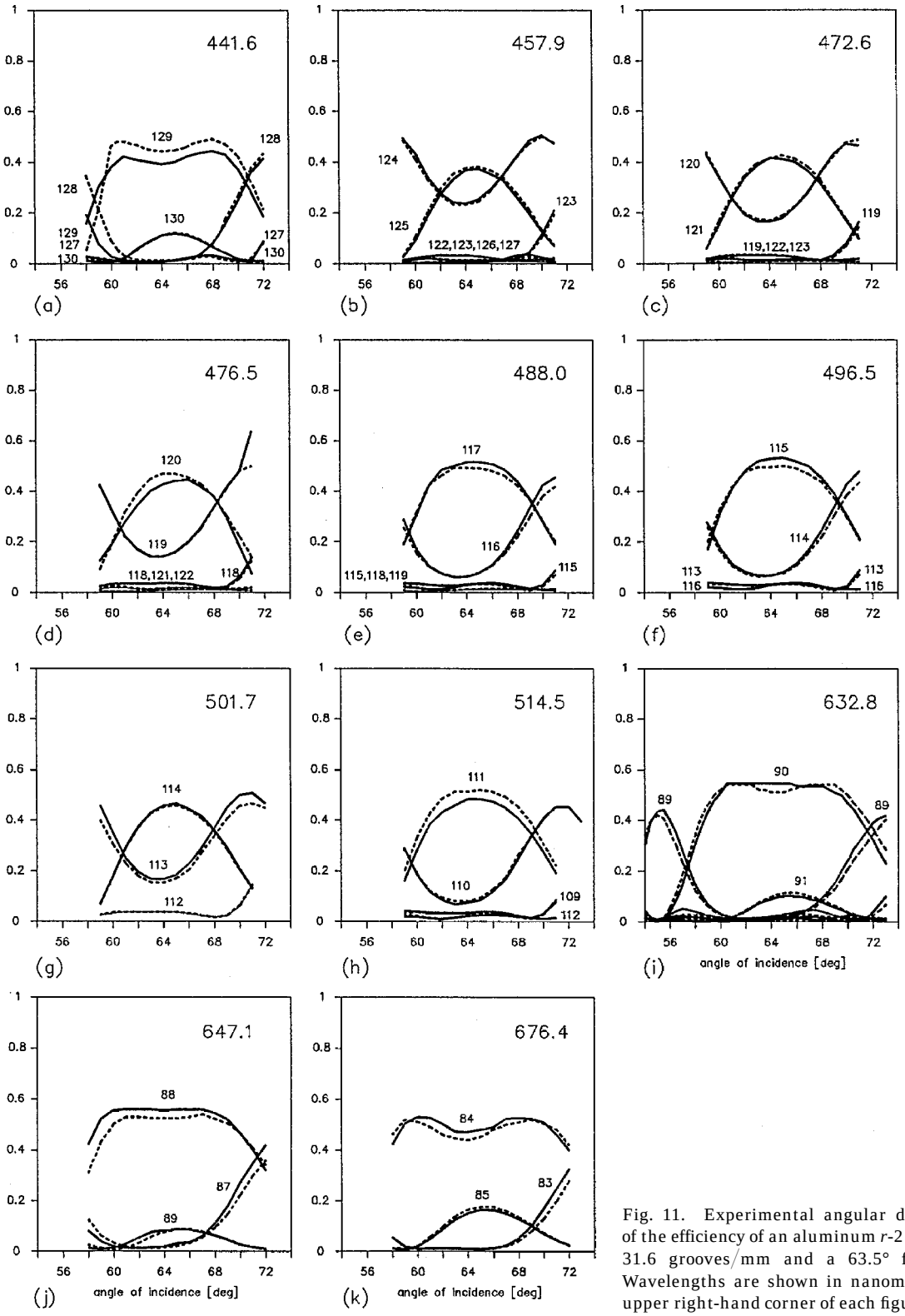

Fig. 11. Experimental angular dependencies of the efficiency of an aluminum *r*-2 echelle with 31.6 grooves/mm and a 63.5° facet angle. Wavelengths are shown in nanometers in the upper right-hand corner of each figure.

647.1 nm, as well as in the orders neighboring the blaze ones: 49 at 488.0 nm and 48 at 496.5 nm. The opposite effect (a small or a large bump) is observed for blaze orders at 488.0 and 676.4 nm. Both effects are too well pronounced, with sharply defined edges, to represent experimental error. The theoretical data fully confirm the existence of the dips and bumps (compare Figs. 13 and 14). In Figs. 13 the edges of the dips and bumps are shown by the vertical markers at the tops of the figures and are identified with the angular limits of diffraction of the neighboring higher order (numbers above the vertical

Table 1. Experimental and Theoretical Values of the Apparent Facet Angle[a] $\tilde{\phi}_B$

		Δ_θ (deg)		$\tilde{\phi}_B$ (deg)		$(\phi_B\ \tilde{\phi}_B)$ (deg)	
λ (μm)	N	Experiment	Theory	Experiment	Theory	Experiment	Theory
0.4416	129	3.5	3.125	64.431	64.334	0.05	0.146
0.4416	128		7.97		64.386		0.095
0.4579	124	5.28	5.82	64.421	64.386	0.06	0.101
0.4579	123		9.25		64.361		0.120
0.4726	120	6.59		64.413		0.07	
0.5017	113	5.52		64.284		0.197	
0.5145	110	6.26		64.315		0.166	
0.6328	89	8.96	8.755	64.260	64.200	0.222	0.281
0.6328	90	2.84	1.88	64.291	64.192	0.190	0.289
0.6471	88	2.386	2.5	64.216	64.226	0.265	0.255
0.6471	87		9.0		64.227		0.254
0.6764	84	4.625	4.625	64.235	64.235	0.246	0.246
0.67906	84		0		64.313		0.168

[a]Obtained from the angular dependencies of an r-2 echelle with 31.6 grooves/mm and a nominal experimental facet angle of 63° 26′. The theoretical facet angle is 64.48°.

markers) in each case. Sometimes, when the efficiency in this order is high enough, its values are also shown in the figures. To the left of the corresponding marker, the next $N + 1$ order cannot diffract, and to the right of marker (-1) the $N - 1$ order cannot diffract. Between them there is a window in which either both or neither can diffract. When they can diffract, they rob light from the main Nth order. The sharpness with which this region is bounded is well known in echelette theory and corresponds to the Wood anomalies, or specifically to the Rayleigh passing-off effect. They seem not to have been previously reported. The role of the cut-off effects can be observed by comparison of Figs. 13(c) with 13(d) and 13(i) with 13(j). With an increasing wavelength, the cutoffs of the $N + 1$ and $N - 1$ orders approach each other. We have traced the evolution theoretically in Fig. 15, both in a large-scale domain with switching between different orders and in a small-scale domain, in which small wavelength changes lead to different cut-off effects within the same order. The passing-off position (at an angle for the Nth-diffracted order) is derived as a direct consequence of the grating equation, given by

$$\sin(\theta_{N_C}) = N\frac{\lambda}{d} - 1, \tag{13}$$

so that the increase of the wavelength moves the $N + 1$ cutoff to higher angles of incidence, for which it is assumed that blazing occurs in the Nth order. The corresponding passing-off position for the -1 order is given by the equation

$$\sin[\theta_{(-1)_C}] = 1 - \frac{\lambda}{d}, \tag{14}$$

and its variation with λ is much slower ($N + 1$ times) than the cutoff of the order $N + 1$, which is a direct consequence of Eqs. (13) and (14). Thus the window

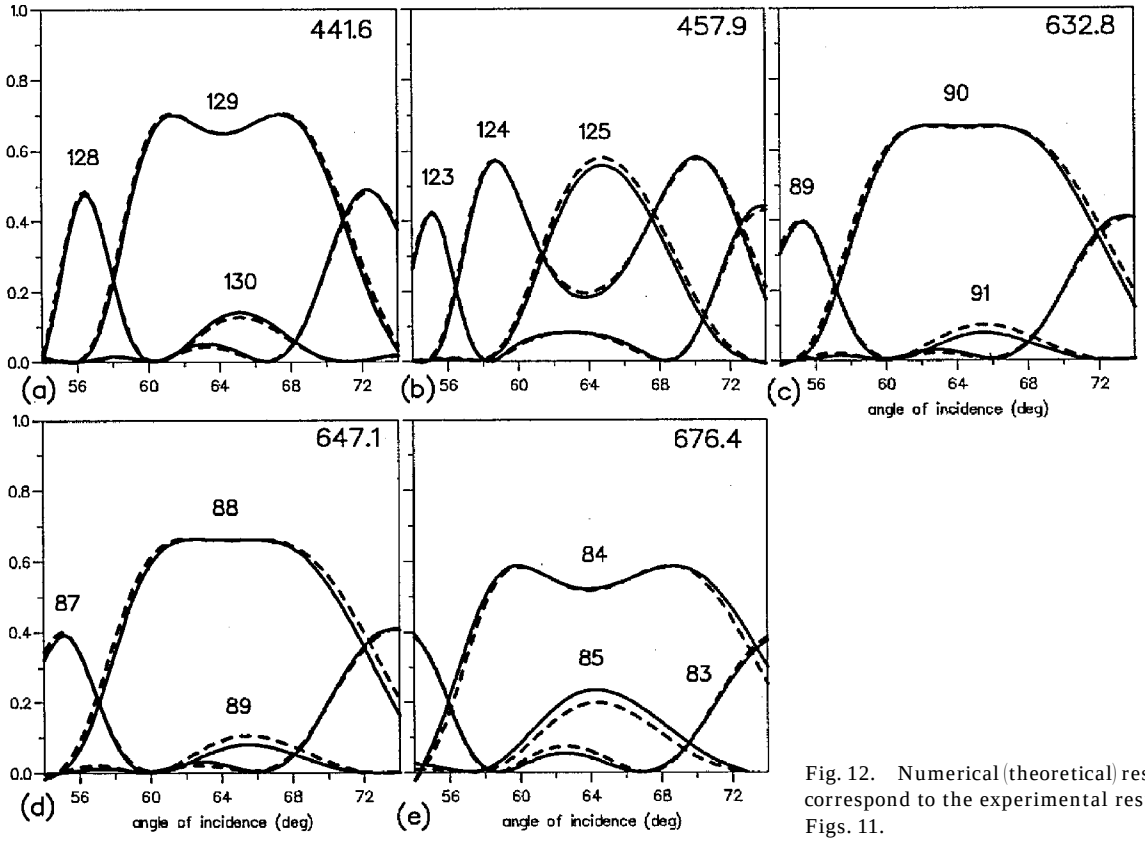

Fig. 12. Numerical (theoretical) results that correspond to the experimental results from Figs. 11.

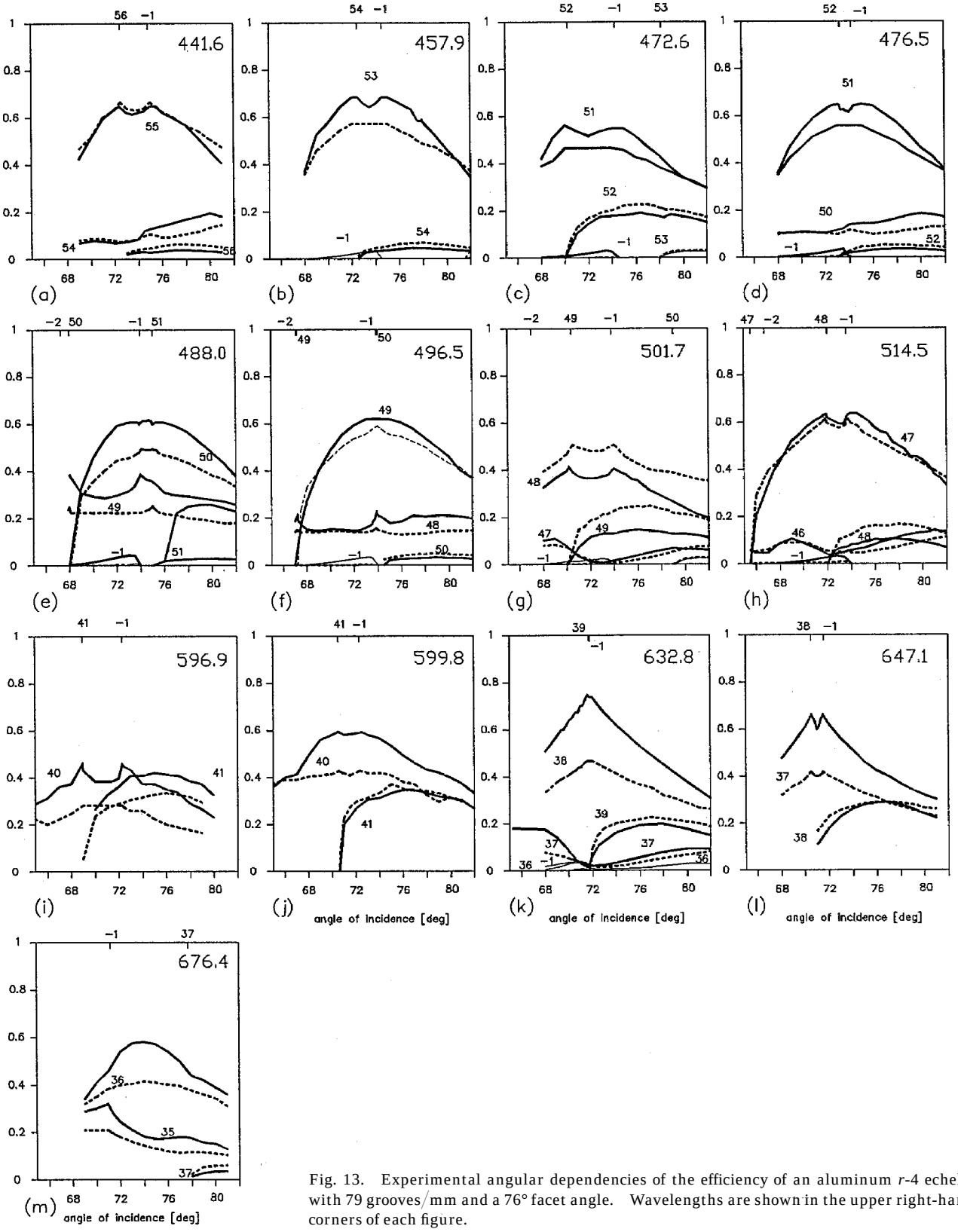

Fig. 13. Experimental angular dependencies of the efficiency of an aluminum *r*-4 echelle with 79 grooves/mm and a 76° facet angle. Wavelengths are shown in the upper right-hand corners of each figure.

width is determined mainly by the passing-off position of the higher order (with respect to the blazing order), as can be easily traced in Fig. 15.

Above some limit at which there are no more $N + 1$ or $N - 1$ orders inside the window to rob light from the main (Nth) order, there will be an efficiency boost, which is clearly observed at 488.0 and 676.4 nm (Figs. 13 and 14). In the latter case (676.4 nm) one would

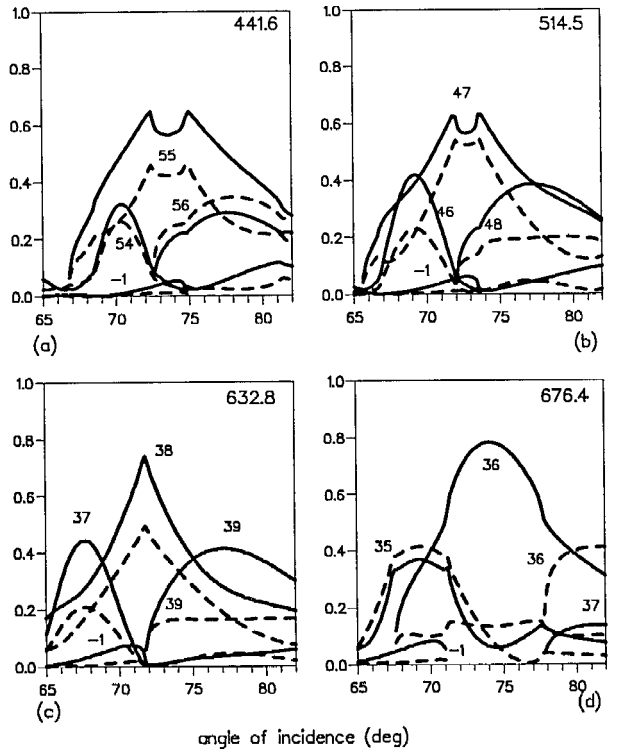

Fig. 14. Numerical (theoretical) results in (a) and (b) correspond to the experimental results from Figs. 13. (c) Refractive index $n = 1.09 + i5.31$, and (d) $n = 1.3 + i7.11$.

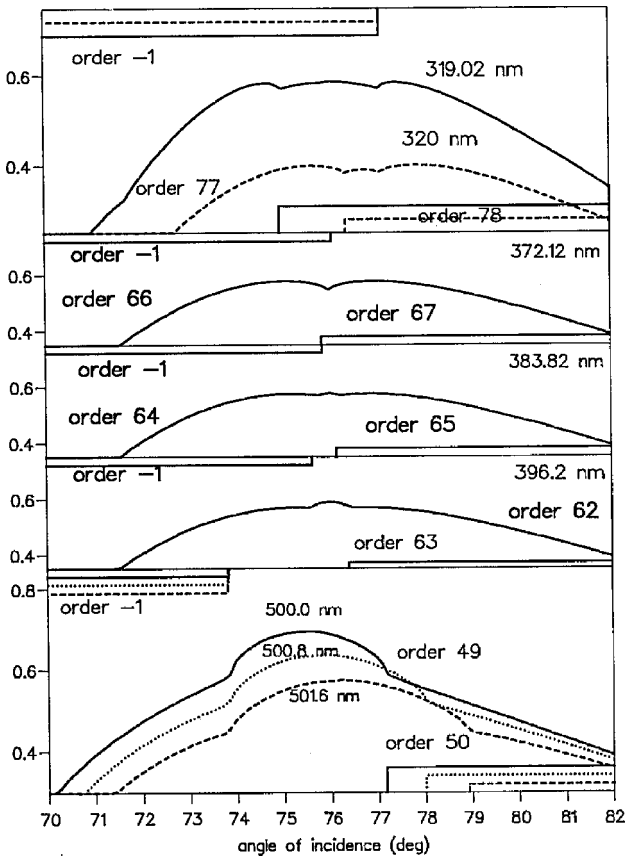

Fig. 15. Numerical investigation of an r-4 echelle with 79 grooves/mm: Influence of the passing-off effect on the −1 order and on the orders adjacent to peak one for several different wavelengths (shown in nanometers). The region in which the −1 order propagates is shown in the rectangular area in the upper part of each graph and the region in which the order next to peak one propagates is marked at the bottom of each graph.

expect a boost to the efficiency in the 36th order, were it not for the circumstance that it corresponds to a fractional order (35.7), so that a significant amount of light goes into the 35th order. When the two orders are combined, their total in the TE plane reaches a rather high value of 90%, while the equivalent value in the TM plane is only 60%. It seems that, when tuned to a different λ/d ratio so that an integer order number appears to be blazing, a higher efficiency can be expected when the neighboring order, and the −1 order as well, cannot propagate. The choice, however, is not so easy to make because the real (observed) blaze position differs from the expected one, especially for lower blaze orders (see Figs. 13). The best fit seems to be observed for the 47th order at 514.5 nm. At this wavelength, the adjacent orders have a low efficiency (<2%) and the polarization effect is low (<10%), but the maximum lies within a window in which both orders 48 and −1 can propagate.

Thus we reach 632.8 nm, which by accident presents the limiting case, when the passing-off positions of both order −1 and order 39 coincide at the blaze peak, which leads to an unusually high TE efficiency peak of 75% in the 39th order and also to the highest observed degree of polarization (23%). This wavelength is interesting because it also provides an example of the largest deviation from scalar expectations. Not only is the polarization degree large, but the shift of the efficiency peak is much greater than what one would expect from Fig. 5. Figure 5 predicts a shift of approximately 4–5 nm from the scalar, ideal blaze wavelength, which is equal to 646.43 nm for a facet angle of 76°, whereas the shift as evaluated from Fig. 13(k) exceeds 14 nm. Arguments of possibly differing experimental facet angles may be true, but they are not sufficient, because theoretical results that are based on an exact 76° facet angle give results similar to the experimental ones. Moreover, the mirror expectations, which can easily explain the saddlelike behavior in high orders, fail to work here. There is no two-peak maximum in Fig. 13(k). The explanation can be found in the role of the 39th order, which reaches almost 20% close to its passing-off position and thus takes energy from the 38th order. The latter exhibits a maximum just close to the angle at which the 39th order disappears. This effect becomes obvious in Figs. 16, in which the solid white curves represent the cut-off limit of the 39th order, to the left of which the order does not propagate. The region with maximum efficiency in the 38th order is pushed to the right in both the TE and TM planes.

Special attention should be paid to comparison between theoretical (Figs. 14) and experimental (Figs. 13) results. Whereas the maximum orders behave

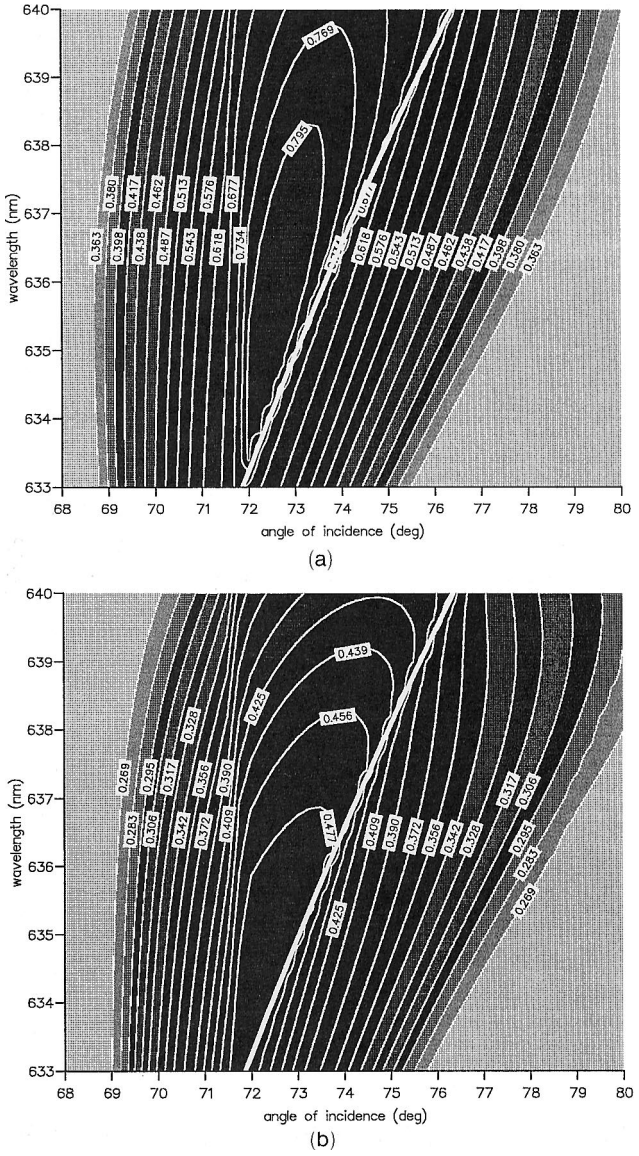

Fig. 16. Numerical results for $n_{A1} = 1.09 + i5.31$. Two-dimensional views of (a) the TE and (b) the TM planes with corresponding isolines and their levels of the diffraction efficiency in the 38th order as a function of the wavelength and angle of incidence for an *r*-4 echelle with 79 grooves/mm and a 76° facet angle [corresponding to Figs. 13(k) and 14(c)].

well for the lower wavelengths, in the red there is a great difference in the TM plane. At 632.8 nm the comparison reveals only some deviations in the values and not in the behavior, but at 676.4 nm the theoretical maximum in the TE plane of the 36th order is accompanied by an unusual minimum in the TM plane. The difference arises from the different values of the aluminum refractive index that was used in the calculations at these two wavelengths. Whereas at 632.8 nm the value of n_{A1} was $1.09 + i5.31$, at 676.4 nm we used the usual bulk value of $1.3 + i7.11$. The effect of this choice is discussed in Section 4.

When a lower facet angle near 63.5° (the *r*-2 echelle) is used, it is evident that passing-off orders no longer play a noticeable role (Figs. 17). This lack comes from so many of these orders propagating between the blaze order and the passing-off order that any cut-off effects are effectively smoothed out. One of the wavelengths (501.7 nm) falls very close to an integer order [45 in Fig. 17(g)], as is evident from the low values of both adjacent orders and the barely detectable level of polarization. At 441.6 nm [Fig. 17(a)] the nominal order is 51.1, which explains why order 52 is stronger. At 496.5 nm we are almost exactly at the half-order position, as is evident by the fact that, near the facet angle, orders 45 and 46 intersect, and their combined value adds up to 60%, which is typical for such a grating. At 632.8 nm the 36th order dominates; adding it to order 35 leads to a combined peak value close to 64%. The lack of passing-off effects allows one to attempt to use Eq. (12) again to reconstruct the observed facet angle from the angular data. The results are summarized in Table 2, together with the approximation of the real facet angle ϕ_B from the apparent one $\tilde{\phi}_B$ from the theoretical data from Fig. 5 and relation (7), with $\delta = 0.6$. The notations are the same as in Table 1. As discussed above, the apparent facet angle $\tilde{\phi}_B$ decreases as the wavelength increases, and the resulting real facet angle ϕ_B (approximately 63.4°) lies close to the nominal one.

3.C. Efficiency Behavior in the Low Orders

The only grating tested in the low-order domain was a 316-grooves-mm echelle with a 63.4° nominal facet angle, which allowed us to test orders of 8–13. In this domain the degree of polarization can be so strong, as much as 40%, that the scalar model clearly cannot apply. The effects of the passing-off orders can become quite strong; this result points to a critical comparison with rigorous theory. In general, good agreement (within two to eight percent) is found in the TE plane. The behavior in the TM plane is also quite well described, even though magnitudes may differ significantly in some instances (this variation is typical of the resonance domain). It must be pointed out that for this grating the small facet does not exceed three wavelengths in width.

If one starts with the shortest wavelength of 441.6 nm [Fig. 18(a)], the nominal order is 12.8, so we can observe nearly equal efficiencies in orders 12 and 13. Between the 54.5° and 59.5° angles of incidence, both the −1 and the 13th orders can diffract; hence they account for the depression in the 12th-order peak. The corresponding theoretical results [Fig. 19(a)] match well in both the TE and TM planes, with the difference not exceeding 10%. At 496.5 nm we are in the 11.4-order position, but we can see no symmetry because the 12th order cannot diffract below 62°. Polarization is at a record 40% [Fig. 18(f)], which is even higher in the theoretical results [Fig. 19(b)]. Compared with the previous case the location of the passing-off orders is reversed in that the −1 order can diffract only below 57.5°. The result is a boost for the 11th order in the window between 57.5° and 62°. At 496.5 and 501.7 nm [Figs. 18(f) and 18(g)] we have

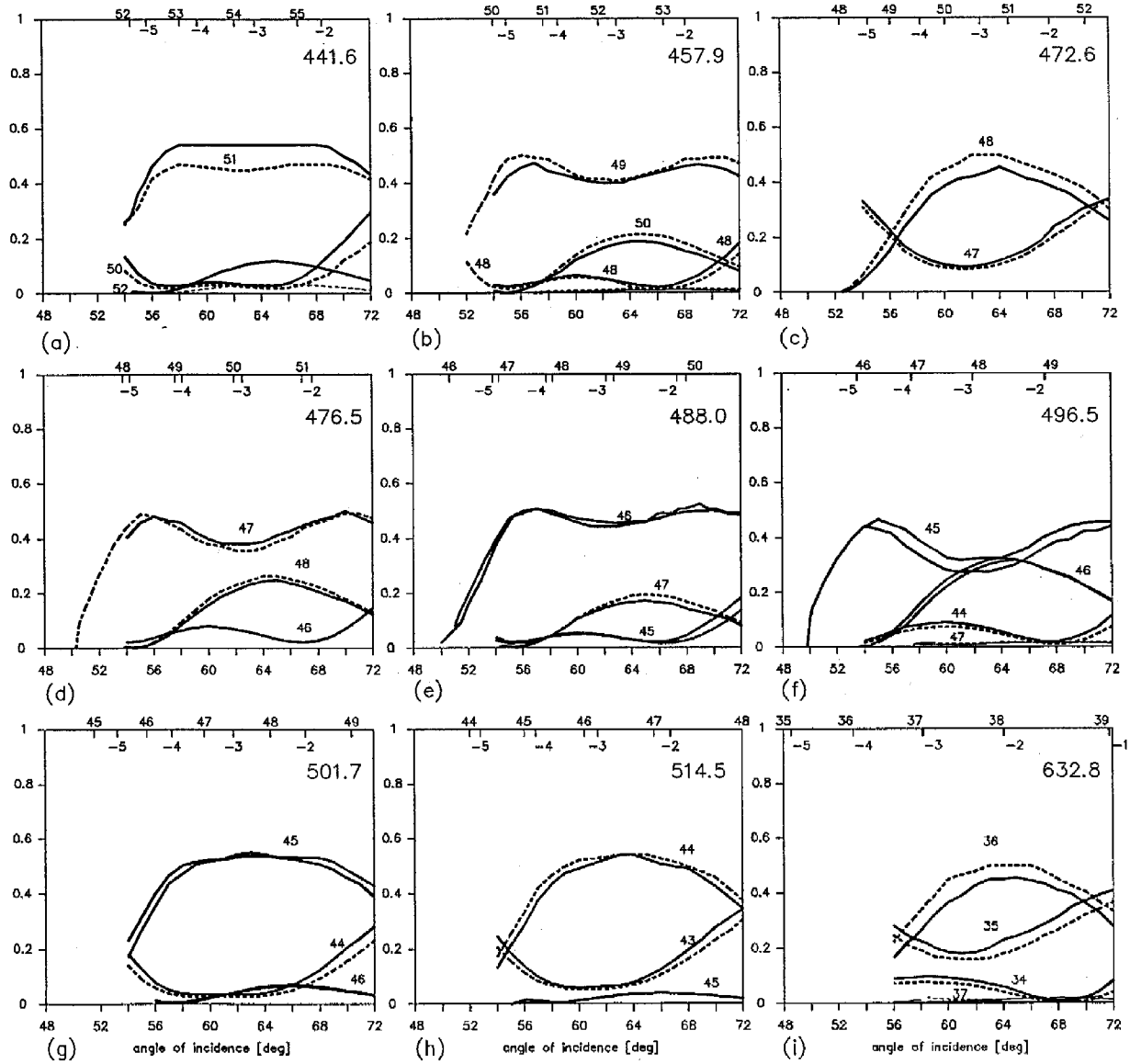

Fig. 17. Experimental angular dependencies of the diffraction efficiency of an *r*-2 echelle with 79 grooves/mm.

a similar effect for the 11th order, and the TM plane again provides lower results. Order 8 in Figs. 18(j) and 18(k) behaves similarly.

At 514.5 nm [Fig. 18(h)] a good order match at order 11 reduces the polarization level. The theoretical results match the experiment well, except for the 10% difference in the TM plane. The evidence of the −1 order's passing off is clear in both orders, but especially in the 10th order. The wavelength 632.8 nm nearly corresponds to the integer order: 8.94. The −1 and 9th orders happen to pass off together, close to 53°, and the effect is visible in order 8. In order 9 the TE curve again matches almost perfectly with the theory [Fig. 19(d)], whereas in the TM plane theory predicts 20% higher values. In order 8 there is a good match in both planes.

Table 2. Experimental Values of the Apparent Facet Angle[a] $\tilde{\phi}_B$

λ (μm)	N	Δ_θ (deg)	$\tilde{\phi}_B$ (deg)	ϕ_B (deg)
0.4416	51	5	63.253	63.56
0.4579	49	7	63.242	63.57
0.4765	47	7	63.033	63.38
0.4880	46	6	63.072	63.43
0.4965	45	8	63.025	63.40
0.6764	33	7	62.660	63.26

[a]Obtained from the angular dependencies of an *r*-2 echelle with 79 grooves/mm and a nominal experimental facet angle of 63° 26′. ϕ_B is the real facet angle and was reconstructed with Eq. (12).

4. Deviations in Groove Parameters and Echelle Performance

4.A. Refractive Index of the Grating Material

One of the main difficulties to the accurate solution of the physics of gratings is that the available refractive indices of the materials with which they are built are

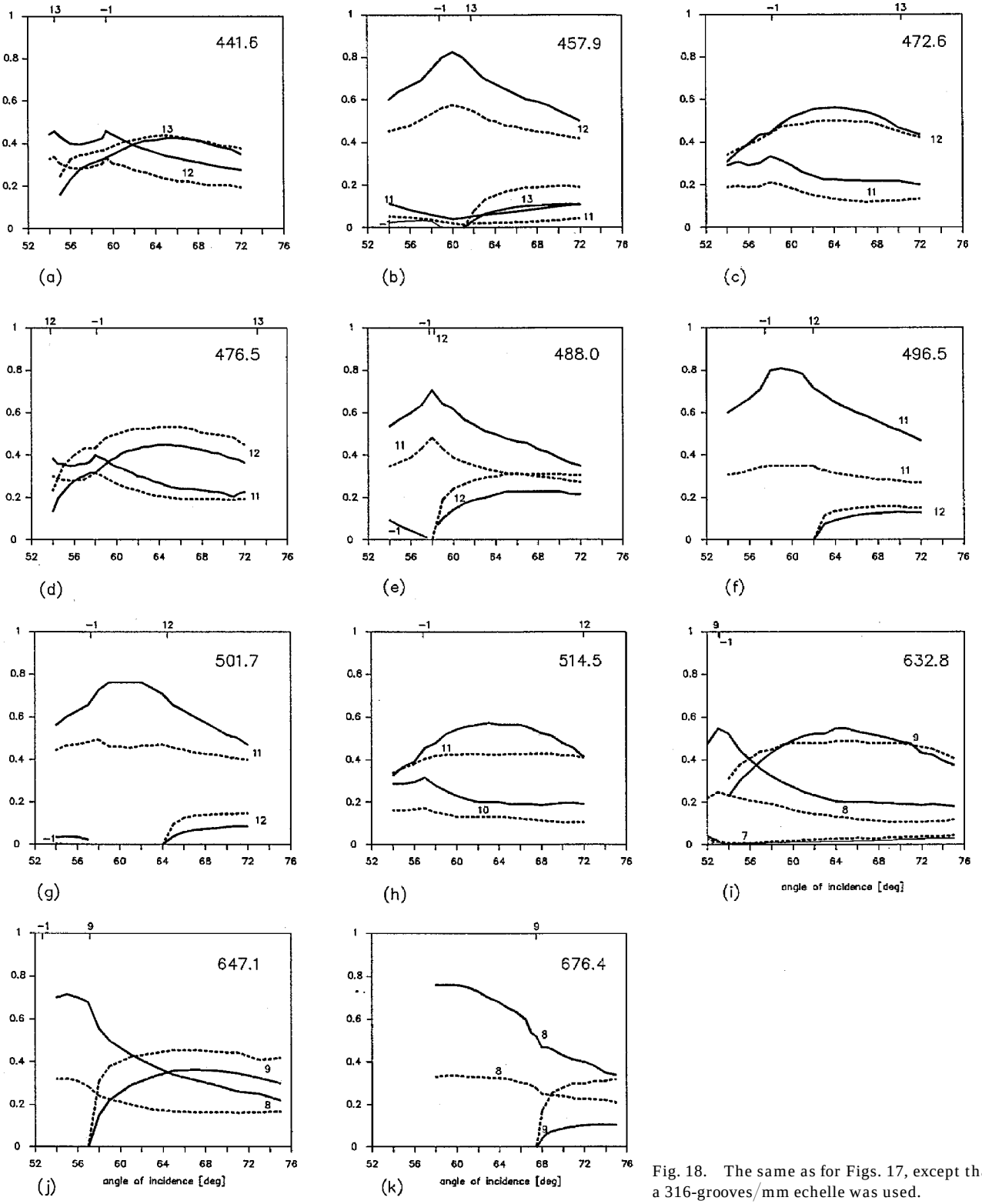

Fig. 18. The same as for Figs. 17, except that a 316-grooves/mm echelle was used.

almost never quite equal to the effective refractive indices. To begin with, properties of thin layers may differ from the properties of bulk material and, unfortunately, in the worse direction: impurities such as nonhomogeneities during layer growth and roughness are introduced. The result is that the reflectivity of the layers is usually lower, and the difference with the bulk polished surface varies more or less with the wavelength. The variation differs not only from one layer-growing device to another but also within one such device under different conditions.

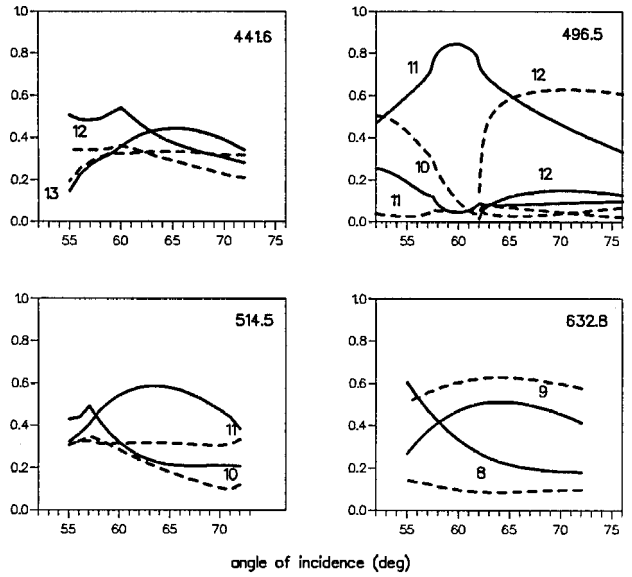

Fig. 19. Numerical values that correspond to the experimental results in Figs. 18.

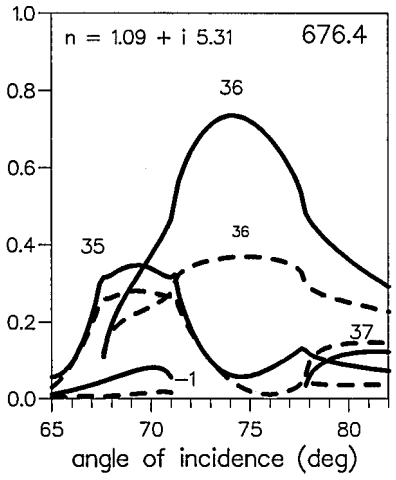

Fig. 20. Numerical results that correspond to Fig. 14(d) ($n = 1.3 + i7.11$) but with a refractive-index value of $n = 1.09 + i5.31$.

The role of this uncertainty can hardly be predicted. A typical set of examples is shown in Figs. 3, with a discussion of the effect of finite conductivity. The bulk textbook value for aluminum in the red is close to $n = 1.20 + i7.00$, but Fig. 3(b) shows that this value leads to a polarization degree much higher than that observed in the experiments. Moreover, the tail near the passing-off positions of the 41st and 42nd orders in TM polarization is quite strong, and we were not able to locate such behavior in any of the experiments (see Figs. 8). It is well known in grating theory that refractive-index values can significantly modify the efficiency behavior in the resonance domain and, in particular, the resonance phenomena (anomalies). As we have already shown throughout the previous section, anomalies do play a role in echelle behavior. To analyze the influence of the refractive index, we completed another set of calculations regarding the echelle from Fig. 3(b) with a refractive index slightly different from the bulk one. Its value, which was taken from another grating study,[22] does not necessarily characterize the echelle-manufacturing process, but it serves as an example of how the index influences echelle behavior. The results shown in Fig. 3(c) are obviously different from the bulk-value results: The tail in the TM plane disappears, and the maximum positions in the TE and TM planes approach each other. The case is similar when Figs. 14(c) and 14(d) are compared with the corresponding experimental data. The former [Fig. 14(c)] is calculated with the assumption of lower values for both the real and imaginary parts of the aluminum refractive index (although this does not mean lower reflectivity values) and matches the experimental data much better than do the high-refractive-index calculations [Figs. 14(d) and 3(b)]. New calculations with the same parameters and wavelengths as were used for the data shown in Fig. 14(d), except for a lower refractive index, give results much closer to the experimental ones (Fig. 20).

4.B. Groove-Angle and Profile Deformations

Grating users may demand an echelle with a specific groove (facet) angle that serves their purposes, but no manufacturer wants to guarantee an accuracy of 0.1°. Although a 0.1° accuracy might seem an excessive demand, Fig. 21 serves as a warning to show that even an 0.08° error in the facet angle can lead to noticeable effects. For the 84th order such a minor

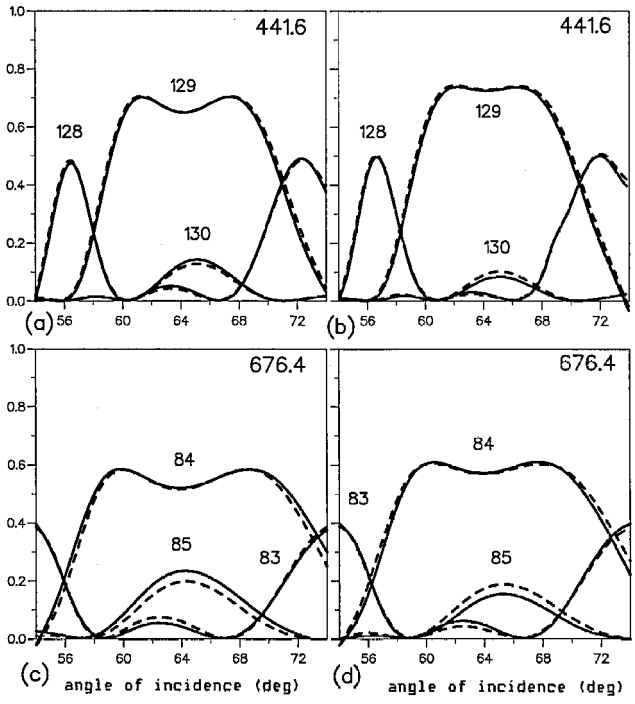

Fig. 21. Numerical comparison of the angular dependencies of the efficiency for a 31.6-grooves/mm r-2 echelle with two slightly different facet angles: 64.481° in (a) and (c), and 64.400° in (b) and (d), for two different wavelength values.

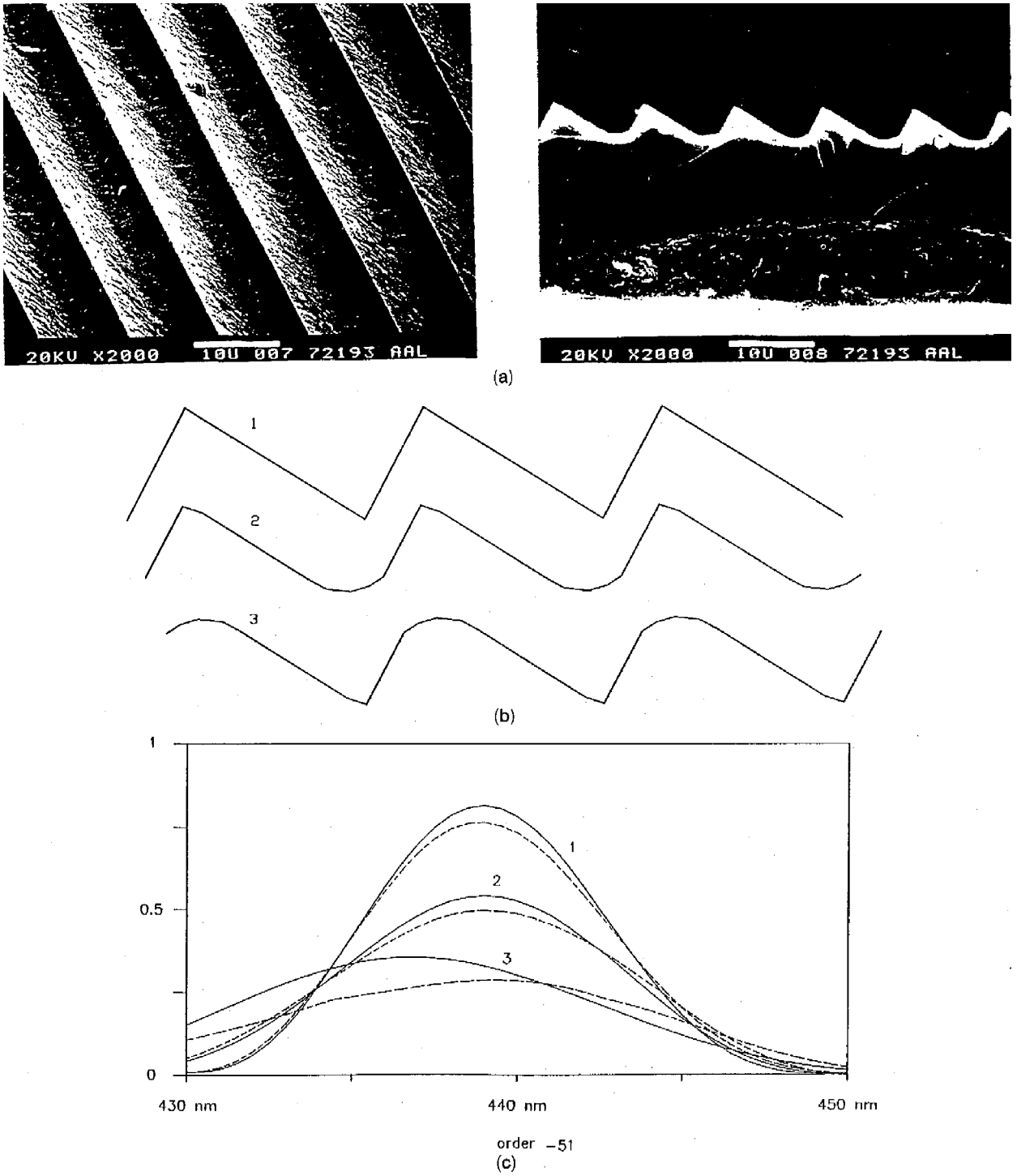

Fig. 22. Representations of an *r*-2 echelle with 79 grooves/mm and a 63.5° facet angle: (a) SEM pictures of a thin-film replica cut in liquid nitrogen: left-hand side, top view; right-hand side, lateral view. (b) Drawings of the reconstructed (2), inverted (3), and ideal (1) profiles of the echelle; the ideal profile has a facet angle of 62.4° and apex angle of 84.2°. (c) Numerically determined spectral dependence of order 51 for profiles 1, 2, and 3 from (b). Solid curves represent TE polarization, and dashed curves represent TM.

error corresponds to 1/17 of the order and leads to an increase of the leakage into order 85 for an echelle with a larger facet angle (64.481° as compared to 64.400°). At 441.6 nm the effect is even greater, the error now being 1/11 of the order separation. The conclusion is that only a coincidence can lead to the achievement of echelles with the exact desired facet angle. For most applications such an error will do no harm.

More important and more difficult to predict can be the effect of material flow during the echelle ruling. Because grooves are formed not by the echelle's being

cut but by severe plastic deformation, the top edge will always appear to be rounded in comparison with the sharp bottom edge [Fig. 22(a) shows a scanning electron microscope (SEM) picture of an inverted replica]. This effect is well known and explains the universal use of odd-generation replicas, for which the groove is inverted and the deformed part lies at the bottom. Theoretical results [Fig. 22(c)] confirm that, when even-generation replicas replace odd ones, the efficiency is much less. The main reason for the lack of a good direct comparison between experimental and theoretical results is that we lacked a set of even and odd replicas from an echelle that had served as an object for SEM pictures and vice versa. A severe difficulty lies in the process of sample preparation for a SEM. Correct groove-function determination is possible only from a picture of the grating-surface cut, which requires a polishing step that unfortunately tends to deform the profile. A possible alternative to this technique would be for one to make a metallic replica without a plastic cover, freeze it in liquid nitrogen, break the thin layer, and take a picture of the cut, hoping not to deform it significantly during the process. Thus Fig. 22(a) is the only picture available. However, even these limited data show that real gratings can differ significantly from ideal echelles and that this difference can visibly change their properties.

5. Conclusion

A detailed theoretical and experimental study of a wide range of echelle gratings has shown the usefulness of newly developed techniques for the numerical study of efficiency behavior. The correlation between theory and experiment has fully established the validity, within limits set by our knowledge of material properties and groove geometry. This has enabled us to determine the boundaries of usefulness of scalar theory, which in the past has been the only model. Unexpected was the discovery that passing-off phenomena, which have long been known for echelette gratings, also play a role for certain echelles. A puzzle of longstanding has been the apparent deviation in blaze-peak direction with wavelength, which was attacked in this paper through numerical techniques. They showed that, as the wavelength decreases, the TE and TM planes of polarization response come closer together according to a power law for which the exponents have been developed.

References

1. G. R. Harrison, "The production of diffraction gratings: II. The design of echelle gratings and spectrographs," J. Opt. Soc. Am. **39,** 522–528 (1949).
2. G. R. Harrison, E. G. Loewen, and R. S. Wiley, "Echelle gratings: their testing and improvement," Appl. Opt. **15,** 971–976 (1976).
3. W. M. Burton and N. K. Reay, "Echelle efficiency measurements in the ultraviolet," Appl. Opt. **9,** 1227–1229 (1970).
4. D. J. Schroeder and R. L. Hillard, "Echelle efficiencies: theory and experiment," Appl. Opt. **19,** 2833–2841 (1980).
5. R. G. Tull, "A comparison of holographic and echelle gratings in astronomical spectrometry," in *Proceedings of the Ninth Workshop on Instrumentation of Ground-Based Optical Astronomy,* L. B. Robinson, ed. (Springer-Verlag, Berlin, 1988), pp. 104–117.
6. D. J. Schroeder, "An echelle spectrometer–spectrograph for astronomical use," Appl. Opt. **6,** 1976–1980 (1967).
7. R. C. M. Learner, "Spectrograph design 1918–68," J. Phys. E **1,** 589–594 (1968).
8. J. Kielkopf, "Echelle and holographic gratings compared for scattering and spectral resolution," Appl. Opt. **20,** 3327–3331 (1981).
9. S. Engman and P. Lindblom, "Multiechelle grating mountings with high spectral resolution and dispersion," Appl. Opt. **21,** 4363–4371 (1982).
10. P. Lindblom and F. Stenman, "Resolving power of multigrating spectrometers," Appl. Opt. **28,** 2542–2549 (1989).
11. M. Bottema, "Echelle efficiencies: theory and experiment; comment," Appl. Opt. **20,** 528–530 (1981).
12. D. J. Schroeder, "Echelle efficiencies: theory and experiment; author's reply to comment," Appl. Opt. **20,** 530–531 (1981).
13. S. Engman and P. Lindblom, "Blaze characteristics of echelle gratings," Appl. Opt. **21,** 4356–4362 (1982).
14. F. Zhao, "A diffraction model for echelle gratings," J. Mod. Opt. **38,** 2241–2246 (1991).
15. J. W. Strutt, "On the dynamical theory of gratings," Proc. R. Soc. London Ser. A **79,** 399–416 (1907).
16. R. Petit, ed., *Electromagnetic Theory of Gratings* (Springer-Verlag, Berlin, 1980).
17. D. Maystre, "Rigorous vector theories of diffraction gratings," in *Progress in Optics,* E. Wolf, ed. (Elsevier, New York, 1984), Vol. 21, pp. 1–67.
18. R. A. Brown, R. L. Hilliard, and A. L. Phillips, "Actual blaze angle of the Bausch & Lomb R4 echelle grating," Appl. Opt. **21,** 167–168 (1982).
19. S. Engman and P. Lindblom, "Blaze angle of the Bausch & Lomb R4 echelle grating," Appl. Opt. **22,** 2512–2513 (1983).
20. M. Born and E. Wolf, *Principles of Optics* (Pergamon, New York, 1959).
21. A. Marechal and G. W. Stroke, "Sur l'origine des effets de polarisation et de diffraction dans les réseaux optiques," C. R. Acad. Sci. **29,** 2042–2044 (1959).
22. L. Mashev and E. Popov, "Reflection gratings in conical diffraction mounting," J. Opt. (Paris) **18,** 3–8 (1987).